Electronic Supplementary Information
for the communication entitled

Synthesis of seminaphtho-phospha-fluorescein dyes based on the consecutive arylation of aryldichlorophosphines

Aiko Fukazawa,*[1] Junichi Usuba,[1] Raúl A. Adler,[2] and Shigehiro Yamaguchi*[1,2]

[1]*Department of Chemistry, Graduate School of Science and Integrated Research Consortium on Chemical Sciences (IRCCS), Nagoya University, Furo, Chikusa, Nagoya 464-8602, Japan*
[2]*Institute of Transformative Bio-Molecules (WPI-ITbM), Nagoya University, Furo, Chikusa, Nagoya 464-8602, Japan*

Contents

1. Experimental Details

General. Melting points (mp) or decomposition temperatures were determined with a Yanaco MP-S3 instrument or a Stanford Research System OptiMelt MPA100 instrument. ^{1}H, $^{13}C\{^{1}H\}$, and $^{31}P\{^{1}H\}$ NMR spectra were recorded with a JEOL AL-400 spectrometer (400 MHz for ^{1}H, 100 MHz for ^{13}C, and 162 MHz for ^{31}P), a JEOL ECS400 spectrometer (400 MHz for ^{1}H and 100 MHz for ^{13}C) or a JEOL ECA 600 II spectrometer equipped with an UltraCOOL probe (150 MHz for ^{13}C) in $CDCl_3$, acetone-d_6, methanol-d_4, or DMSO-d_6. The chemical shifts in ^{1}H NMR spectra are reported in δ ppm using the residual protons of the solvents as an internal standard ($CHCl_3$ δ 7.26, acetone δ 2.05, methanol δ 3.31, DMSO δ 2.50), and those in ^{13}C NMR spectra are reported using the solvent signals as an internal standard ($CDCl_3$ δ 77.16, methanol-d_4 δ 49.00, DMSO-d_6 δ 39.52). The chemical shifts in ^{31}P NMR spectra are reported using H_3PO_4 (δ 0.00) as an external standard. Mass spectra were measured with a JEOL JMS 700 (FAB), a Bruker micrOTOF Focus spectrometry system with the ionization method of APCI, or a ThermoFisher Scientific Exactive with the ionization method of ESI. Thin layer chromatography (TLC) was performed on glass plates coated with 0.25 mm thickness of silica gel $60F_{254}$ (Merck). Preparative thin layer chromatography (PTLC) was performed on glass plates coated with 1.0 mm thickness of silica gel EMD Millipore 1.13895.0001 (Merck). Column chromatography was performed using silica gel PSQ100B or PSQ60B (Fuji Silysia Chemicals). Recycling preparative HPLC was performed using YMC LC-forte/R equipped with a silica gel column (YMC-Actus SIL). All reactions were performed under a nitrogen atmosphere unless stated otherwise. Commercially available solvents and reagents were used without further purification unless otherwise mentioned. Anhydrous THF were purchased from Kanto Chemicals and further purified by Glass Contour Solvent Systems.

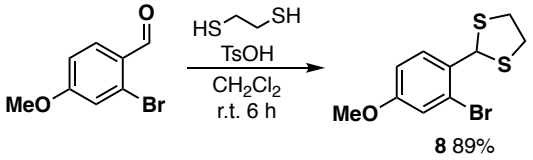

Scheme S1. Synthesis of **8**.

2-(2-Bromo-4-methoxyphenyl)-1,3-dithiolane (8). To a solution of 2-bromo-4-methoxybenzaldehyde (1.91 g, 8.88 mmol) and $TsOH{\cdot}H_2O$ (242 mg, 1.27 mmol) in CH_2Cl_2 (25 mL) was added 1,2-ethanedithiol (1.2 mL, 1.35 g, 14.3 mmol) at ambient temperature in air. After stirring for 6 h at the same temperature, the mixture was transferred into a separatory funnel and washed with water three times. The organic layer was dried over anhydrous Na_2SO_4, filtered, and concentrated under reduced pressure. The resulting yellow oil was subjected to silica gel column chromatography (PSQ100B, 5/1 hexane/ethyl acetate as an eluent, R_f = 0.50) to afford 2.30 g (7.90 mmol, 89% yield) of **8** as colorless oil: ^{1}H NMR (400 MHz, $CDCl_3$): δ 3.32–3.39 (m, 2H), 3.43–3.50 (m, 2H), 6.03 (s, 1H), 3.79 (s, 3H), 6.86 (dd, J = 8.8, 2.6 Hz, 1H), 7.06 (d, J = 2.6 Hz, 1H), 7.76 (d, J = 8.8 Hz, 1H). $^{13}C\{^{1}H\}$ NMR (100 MHz, $CDCl_3$): δ 39.9 (CH_3), 54.8 (CH_2), 55.7(CH), 114.2 (CH), 117.7(CH), 124.1(C), 130.2 (C), 131.9 (C), 159.5 (C). HRMS (FAB): m/z calcd. for $C_{10}H_{12}{}^{79}BrOS_2$:

290.9507 ([*M*+H]$^+$); found. 290.9516.

A Typical Procedure for the Consecutive Diarylation of $PhPCl_2$: Synthesis of 4-Methoxy-2-[(3-methoxyphenyl)(phenyl)phosphoryl]benzaldehyde (2a). To a solution of 3-bromoanisole (1.73 g, 9.25 mmol) in THF (50 mL) was added *n*-BuLi in hexane (1.60 M, 5.80 mL, 9.28 mmol) dropwise at –78 °C. After stirring for 1 h at the same temperature, a solution of $ZnCl_2$(tmeda) (2.33 g, 9.23 mmol) in THF (60 mL) was added dropwise at the same temperature, and the mixture was allowed to warm to ambient temperature followed by stirring for 1 h. Then, $PhPCl_2$ (1.50 mL, 1.98 g, 11.1 mmol) was added dropwise into the mixture at –78 °C. The mixture was allowed to warm to ambient temperature. After stirring for 18 h, all volatiles were removed under reduced pressure, and hexane (40 mL) was added to the mixture. The resulting suspension was filtered under a N_2 atmosphere, and the filtrate was concentrated under reduced pressure to give a crude chloro(3-methoxyphenyl)(phenyl)phosphine (**4a**).

A solution of **8** (2.81 g, 9.65 mmol) in THF (120 mL) was prepared in another flask, to which was added *n*-BuLi in hexane (1.60 M, 6.10 mL, 9.76 mmol) dropwise at –98 °C. After stirring for 5 min, crude **4a** was added dropwise at the same temperature. After stirring for 3 h at the same temperature, the mixture was allowed to warm to ambient temperature and stirred for another 1 h. Then, an aqueous solution of H_2O_2 (30%, 3.5 mL) was added to the mixture at 0 °C followed by stirring for 30 min at the same temperature. A saturated aqueous solution of Na_2SO_3 (15 mL) was added and the mixture was extracted with CH_2Cl_2. The combined organic layer was washed with brine, dried over anhydrous Na_2SO_4, and filtered. Concentration of the filtrate under reduced pressure afford 3.91 g of crude **5a** as colorless solids.

To a solution of crude **5a** in EtOH (300 mL), a solution of $AgNO_3$ (8.27 g, 48.7 mmol) in water (30 mL) was added at ambient temperature in air. After stirring for 12 h, the mixture was concentrated under reduced pressure. After addition of CH_2Cl_2, the resulting suspension was filtered and washed with CH_2Cl_2. After concentration of the filtrate under reduced pressure, the resulting solids were subjected to a silica gel column chromatography (PSQ100B, 1/1 hexane/acetone as an eluent, R_f = 0.47) to afford 1.58 g (4.31 mmol, 47% yield based on 3-bromoanisole) of **2a** as pale yellow viscous oil: ^{1}H NMR (400 MHz, acetone-d_6): δ 3.825 (s, 1H), 3.829 (s, 3H), 6.73 (dd, J = 15.0, 2.4 Hz, 1H), 7.17–7.23 (m, 2H), 7.28 (ddd, 1H, J = 13.4, 2.6, 1.6 Hz), 7.33 (dd, J = 15.0, 2.4 Hz, 1H), 7.51 (ddd, J = 8.0, 8.0, 3.6 Hz, 1H), 7.55–7.65 (m, 2H), 7.65–7.75 (m, 3H), 8.12 (dd, J = 8.4, 4.4 Hz, 1H), 10.63 (s, 1H). ^{13}C{^{1}H} NMR (100 MHz, $CDCl_3$): δ 55.4 (s, CH_3), 55.6 (s, CH_3), 116.0 (d, $J_{P–C}$ = 2.5 Hz, CH), 116.6 (d, $J_{P–C}$ = 11.6 Hz, CH), 118.3 (d, $J_{P–C}$ = 2.5 Hz, CH), 120.6 (d, $J_{P–C}$ = 11.5 Hz, CH), 123.9 (d, $J_{P–C}$ = 10.7 Hz, CH), 128.7 (d, $J_{P–C}$ = 12.3 Hz, CH), 129.9 (d, $J_{P–C}$ = 13.9 Hz, CH), 131.6 (d, $J_{P–C}$ = 50.3 Hz, CH), 131.72 (d, $J_{P–C}$ = 76.6 Hz, C), 131.73 (d, $J_{P–C}$ = 9.9 Hz, CH), 132.4 (d, $J_{P–C}$ = 2.5 Hz, CH), 132.6 (d, $J_{P–C}$ = 43.7 Hz, C), 133.0 (d, $J_{P–C}$ = 170.4 Hz, C), 137.1 (d, $J_{P–C}$ = 94.6 Hz, C), 159.7 (d, $J_{P–C}$ = 14.8 Hz, C), 162.7 (d, $J_{P–C}$ = 14.8 Hz, C), 189.8 (d, $J_{P–C}$ = 4.9 Hz, CH). ^{31}P{^{1}H} NMR (162 MHz, $CDCl_3$): δ 31.5. HRMS (APCI): *m*/*z* calcd. for $C_{21}H_{20}O_4P$: 367.1094 ([*M*+H]$^+$); found. 367.1089.

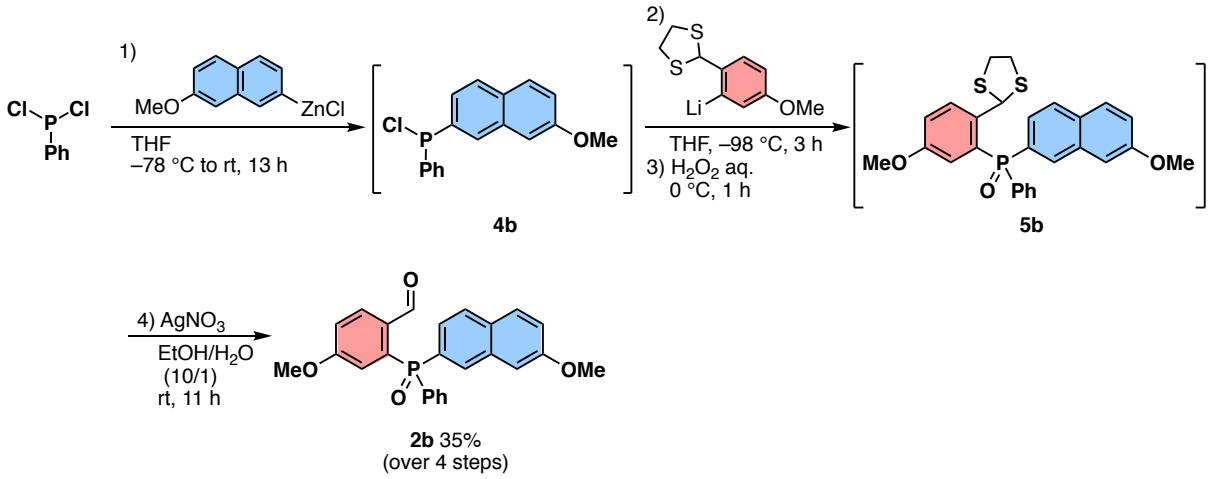

Scheme S2. Synthesis of naphthyl-substituted analogue **2b** via consecutive arylation of $PhPCl_2$.

4-Methoxy-2-[(7-methoxynaphthalen-2-yl)(phenyl)phosphoryl]benzaldehyde (2b). This compound was prepared in a similar manner as described for **2a** using 2-bromo-7-methoxynaphthalene (1.60 g, 6.75 mmol) as a starting material. Purification by the silica gel column chromatography (2/1 to 1/1 hexane/acetone as an eluent, R_f = 0.38 in 1/1 hexane/acetone) afforded 997 mg of **2b** (2.39 mmol, 35% yield based on 2-bromo-7-methoxynaphthalene) as colorless solids: Mp (MPA100): 122.4–123.7 °C. ^{1}H NMR (400 MHz, acetone-d_6): δ 3.81 (s, 3H), 3.93 (s, 3H), 6.79 (dd, J = 15.2, 2.4 Hz, 1H), 7.31 (dd, J = 9.2, 2.4 Hz, 1H), 7.34 (dd, J = 9.2, 2.4 Hz, 1H), 7.44 (d, J = 2.4 Hz, 1H), 7.56–7.67 (m, 4H), 7.75–7.80 (m, 2H), 7.93 (d, J = 8.8 Hz, 1H), 8.01 (dd, J = 8.2, 2.8 Hz, 1H), 8.13 (dd, J = 8.4, 4.4 Hz, 1H), 8.24 (d, J = 14.0 Hz, 1H), 10.63 (s, 1H). ^{13}C NMR (100 MHz, $CDCl_3$): δ 55.4 (CH_3), 55.7 (CH_3), 106.6 (CH), 116.1 (d, $J_{P–C}$ = 2.2 Hz, CH), 120.8 (d, $J_{P–C}$ = 12.1 Hz, CH), 121.7 (CH), 124.4 (d, $J_{P–C}$ = 10.5 Hz, C), 128.4 (d, $J_{P–C}$ = 12.7 Hz, CH), 128.9 (d, $J_{P–C}$ = 12.1 Hz, CH), 129.4 (d, $J_{P–C}$ = 1.1 Hz, CH), 129.8 (d, $J_{P–C}$ = 55.2 Hz, C), 130.4 (d, $J_{P–C}$ = 1.6 Hz, C), 131.9 (d, $J_{P–C}$ = 9.2 Hz, CH), 132.1 (d, $J_{P–C}$ = 30.8 Hz, CH), 132.2 (d, $J_{P–C}$ = 27.0 Hz, CH), 132.3 (d, $J_{P–C}$ = 6.6 Hz, C), 132.5 (CH), 132.3 (d, $J_{P–C}$ = 104.1 Hz, C), 133.8 (d, $J_{P–C}$ = 13.8 Hz, C), 137.4 (d, $J_{P–C}$ = 93.1 Hz, C), 158.5 (d, $J_{P–C}$ = 1.1 Hz, C), 162.8 (d, $J_{P–C}$ = 14.3 Hz, C), 190.0 (d, $J_{P–C}$ = 5.6 Hz, CH). ^{31}P{^{1}H} NMR (162 MHz, $CDCl_3$): δ 31.7. HRMS (APCI): m/z calcd. for $C_{25}H_{22}O_4P$: 417.1250 ($[M+H]^+$); found. 417.1259.

A Typical Procedure for Synthesis of Cyclic Triarylphosphine Oxides 6 via the Nucleophilic Addition and Intramolecular Friedel–Crafts Cyclization: Synthesis of 3,7-dimethoxy-10-(2-methylphenyl)-5-phenyl-10*H*-acridophosphine 5-oxide (*trans*-6aa-Me). To a solution of **2a** (971 mg, 2.65 mmol) in THF (20 mL), was added a solution of *o*-tolylmagnesium bromide in THF (1.62 M, 6.0 mL, 9.72 mmol) dropwise at –78 °C. After stirring for 2 h at the same temperature, the mixture was allowed to warm up to ambient temperature followed by addition of 1*N* HCl aqueous solution (20 mL). After addition of CH_2Cl_2, the layers were separated, and the aqueous layer was extracted with CH_2Cl_2 three times. The combined organic layers were washed with water, dried over anhydrous Na_2SO_4, filtered, and concentrated under reduced pressure to give 1.59 g of

crude **3a-Me** as colorless solids. After dissolving the crude **3a-Me** in toluene (100 mL), $TsOH \cdot H_2O$ (1.52 g, 7.99 mmol) was added, and the resulting suspension was heated at 100 °C for 4 h. After addition of a saturated $NaHCO_3$ aqueous solution (100 mL) at ambient temperature, the mixture was extracted with CH_2Cl_2, and the combined organic layers were dried over anhydrous $MgSO_4$, and concentrated under reduced pressure. The brown mixture was subjected to silica gel column chromatography (PSQ60B, 2/1 to 1/1 hexane/acetone as an eluent, R_f = 0.34 in 1/1 hexane/acetone) to afford 438 mg of *trans*-**6aa-Me** (0.994 mmol, 38% yield based on **2a**) as colorless solids: Mp (MP-S3): 181.2 °C–183.1 °C (dec). ^{1}H NMR (400 MHz, $CDCl_3$): δ 1.81 (s, 1H), 3.85 (s, 6H), 5.12 (d, J_{P-H} = 3.6 Hz, 1H), 6.83 (ddd, J = 8.8, 6.2, 0.4 Hz, 2H), 6.92 (dd, J = 8.8, 3.2 Hz, 2H), 7.19–7.28 (m, 4H), 7.31–7.39 (m, 2H), 7.41–7.50 (m, 3H), 7.65 (dd, J = 13.2, 2.4 Hz, 2H). ^{13}C{^{1}H} NMR (100 MHz, $CDCl_3$): δ 20.3 (s, CH_3), 113.5 (d, J_{P-C} = 7.8 Hz, C), 119.7 (s, CH), 126.7 (s, CH), 127.7 (d, J_{P-C} = 2.5 Hz, CH), 128.6 (d, J_{P-C} = 99.5 Hz, C), 128.8 (d, J_{P-C} = 12.3 Hz, CH), 130.1 (d, J_{P-C} = 11.8 Hz, C), 130.7 (d, J_{P-C} = 10.6 Hz, CH), 132.0 (s, CH), 132.3 (s, CH), 134.8 (d, J_{P-C} = 105.9 Hz, C), 136.5 (d, J_{P-C} = 2.5 Hz, C), 137.2 (s, C), 141.0 (s, C), 158.5 (d, J_{P-C} = 13.4 Hz, C). ^{31}P{^{1}H} NMR (162 MHz, $CDCl_3$): δ 10.6. HRMS (APCI): *m*/*z* calcd. for $C_{28}H_{26}O_3P$: 441.1614 ([*M*+H]$^+$); found. 441.1625.

3,7-Dimethoxy-10-(2,6-dimethylphenyl)-5-phenyl-10*H*-acridophosphine 5-oxide (*trans*-6aa-Me$_2$). This compound was prepared in a similar manner as described for *trans*-**6aa-Me** using **2a** (233 mg, 0.635 mmol) and 2,6-dimethylphenylmagnesium bromide (0.838 M, 2.3 mL, 1.93 mmol) as a starting material. Purification by the silica gel column chromatography (2/1 to 1/1 hexane/acetone as an eluent, R_f = 0.58 in 1/1 hexane/acetone) afforded 66.4 mg of *trans*-**6aa-Me$_2$** (0.146 mmol, 23% yield based on **2a**) as colorless solids: Mp (MP-S3): 181.2 °C–182.8 °C (dec.). ^{1}H NMR (400 MHz, $CDCl_3$): δ 1.41 (s, 3H), 2.35 (s, 3H), 3.87 (s, 6H), 5.40 (d, J_{P-H} = 4.4 Hz, 1H), 6.76 (ddd, J = 8.8, 6.0, 0.8 Hz, 2H), 6.91 (dd, J = 8.8, 2.8 Hz, 2H), 7.02 (dd, J = 6.4, 2.8 Hz, 1H), 7.19–7.26 (m, 2H), 7.35–7.46 (m, 5H), 7.72 (dd, J = 13.2, 2.8 Hz, 2H). ^{13}C{^{1}H} NMR(100 MHz, $CDCl_3$): δ 21.0 (d, J_{P-C} = 3.3 Hz, CH_3), 43.5 (d, J_{P-C} = 8.3 Hz, CH_3), 55.8 (s, CH), 113.5 (d, J_{P-C} = 6.6 Hz, CH), 119.9 (d, J_{P-C} = 2.5 Hz, CH), 127.5 (s, C), 128.9 (s, CH), 128.3 (s, CH), 128.8 (d, J_{P-C} = 12.4 Hz, C), 129.0 (d, J_{P-C} = 11.5 Hz, CH), 130.3 (d, J_{P-C} = 9.8 Hz, CH), 130.8 (s, CH), 131.6 (d, J_{P-C} = 3.3 Hz, CH), 134.7 (s, C), 136.0 (d, J_{P-C} = 8.2 Hz, C), 137.7 (s, C), 138.3 (s, C), 139.3 (s, C), 158.6(d, J_{P-C} = 7.8 Hz, C). ^{31}P{^{1}H} NMR (162 MHz, $CDCl_3$): δ 11.2. HRMS (APCI): *m*/*z* calcd. for $C_{29}H_{28}O_3P$: 445.1771 ([*M*+H]$^+$); found. 445.1750.

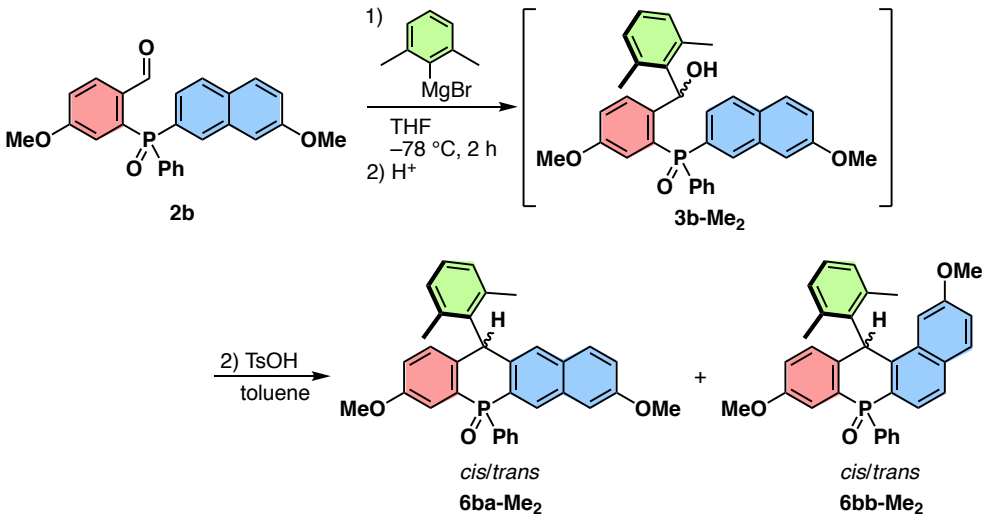

Scheme S3. Friedel–Crafts cyclization of *in-situ* generated **3b-Me$_2$**.

12-(2,6-Dimethylphenyl)-3,8-dimethoxy-5-phenyl-12*H*-benzo[*b*]acridophosphine 5-oxide (*trans*-6ba). This compound was prepared in a similar manner as described for *trans*-**6aa-Me** using **2b** (79.4 mg, 0.191 mmol) and 2,6-dimethylphenylmagnesium bromide (0.838 M, 0.70 mL, 0.587 mmol) as a starting material. Purification by the silica gel column chromatography (2/1 to 1/1 hexane/acetone as an eluent, R_f = 0.59 in 1/1 hexane/acetone) afforded 36.9 mg of *trans*-**6ba-Me$_2$** (73.1 μmol, 38% yield based on **2b**) as colorless solids: Mp (MP-S3): 132.9 °C–134.8 °C. ^{1}H NMR (400 MHz, acetone-d_6): δ 1.47 (s, 3H), 2.30 (s, 3H), 3.90 (s, 3H), 3.96 (s, 3H), 6.80 (dd, J = 8.2, 6.0 Hz, 1H), 7.05 (dd, J = 9.0, 3.2 Hz, 1H), 7.13 (d, J = 4.0 Hz, 1H), 7.20 (dd, J = 8.8, 2.4 Hz, 1H), 7.25–7.28 (m, 3H), 7.35–7.50 (m, 5H), 7.56 (d, J = 2.4 Hz, 1H), 7.63 (d, J = 9.2 Hz, 1H), 7.77 (dd, J = 13.2, 2.8 Hz, 1H), 8.72 (d, J = 13.6 Hz, 1H). ^{13}C{^{1}H} NMR(100 MHz, $CDCl_3$) : δ 21.3 (d, $J_{P–C}$ = 79.9 Hz, CH_3), 44.0 (d, $J_{P–C}$ = 7.4 Hz, CH_3), 55.5 (CH_3), 55.8 (CH_3), 105.9 (C), 113.7 (CH), 113.8 (CH), 119.8 (d, $J_{P–C}$ = 2.4 Hz, CH), 121.4 (CH), 125.8 (d, $J_{P–C}$ = 9.9 Hz, CH), 126.5 (d, $J_{P–C}$ = 98.8 Hz, C), 127.6 (CH), 128.4 (CH), 128.8 (d, $J_{P–C}$ = 12.4 Hz, CH), 128.9 (d, $J_{P–C}$ = 14.9 Hz, CH), 128.9 (d, $J_{P–C}$ = 88.9 Hz, C), 129.6 (CH), 130.5 (d, $J_{P–C}$ = 10.7 Hz, CH), 130.7 (C), 130.7 (CH), 131.2 (d, $J_{P–C}$ = 5.7 Hz, CH), 131.6 (d, $J_{P–C}$ = 3.3 Hz, CH), 132.9 (d, $J_{P–C}$ = 12.3 Hz, C), 135.1 (d, $J_{P–C}$ = 106.1 Hz, C), 136.0 (d, $J_{P–C}$ = 8.2 Hz, C), 136.6 (d, $J_{P–C}$ = 11.2 Hz, C), 138.0 (C), 138.4 (C), 138.6 (C), 158.2 (C), 158.7 (d, $J_{P–C}$ = 13.2 Hz, C). ^{31}P{^{1}H} NMR (162 MHz, $CDCl_3$): δ 10.8. HRMS (APCI): *m*/*z* calcd. for $C_{33}H_{30}O_3P$: 505.1927([*M*+H]$^+$); found. 505.1902.

Separation and Identification of the Isomers Obtained by the Friedel–Crafts Cyclization. To gain insights into the ratio of regioisomers and diastereomers produced by the Friedel–Crafts cyclization of **3aa-Me**, all the isomers, *cis*- and *trans*-**6aa-Me** as well as *cis*- and *trans*-**6ab-Me**, were isolated according to the following procedure: the reaction was conducted in a similar manner as described above using **2a** (65.0 mg, 0.177 mmol) and *o*-tolylmagnesium bromide (1.62 M in THF, 0.33 mL, 0.532 mmol) as a starting material. The crude mixture after aqueous workup was subjected to recycling preparative HPLC (1/1 hexane/Et_2O containing 5% (v/v) MeOH) to afford analytically pure

trans-**6aa-Me** (31.9 mg, 72.4 μmol, 41%) and *cis*-**6ab-Me** (7.5 mg, 17 μmol, 10%) as colorless solids, and the other fraction containing *cis*-**6aa-Me** and *trans*-**6ab-Me**. This fraction was further subjected to PTLC (1/3 hexane/acetone) to afford *cis*-**6aa-Me** (R_f = 0.50, 4.3 mg, 9.8 μmol, 6% yield) and *trans*-**6ab-Me** (R_f = 0.65, 10.3 mg, 23.4 μmol, 13% yield), respectively, as slightly yellowish solids. The structures of *trans*-**6aa-Me** and *cis*-6**ab-Me** were identified unequivocally by X-ray crystallographic analyses (see pp. S10–S12). The structures of the other two isomers *cis*-**6aa-Me** and *trans*-**6ab-Me** were identified by ^{1}H, ^{13}C, and ^{31}P NMR spectroscopy.

***cis*-6aa-Me.** Mp (MP-S3): 94.0–99.5 °C. ^{1}H NMR (400 MHz, $CDCl_3$): δ 2.14 (s, 3H, CH_3), 3.70 (s, 6H, OCH_3), 5.72 (d, $^4J_{P-H}$ = 4.2 Hz, 1H, $HCAr_3$), 6.90–6.91 (m, 4H), 7.01–7.02 (m, 1H), 7.09–7.17 (m, 3H), 7.21–7.24 (m, 2H), 7.47–7.58 (m, 3H), 7.78–7.83 (m, 2H). ^{13}C{^{1}H} NMR (100 MHz, $CDCl_3$) δ 20.4 (s), 46.9 (d, J_{P-C} = 8.3 Hz), 55.5 (s), 114.7 (d, J_{P-C} = 9.6 Hz), 119.7 (d, J_{P-C} = 2.4 Hz), 126.9 (s), 127.5 (s), 128.7 (d, J_{P-C} = 12.4 Hz), 129.0 (d, J_{P-C} = 102.0 Hz), 130.9 (d, J_{P-C} = 10.8 Hz), 131.8 (s), 131.9 (s), 132.1 (d, J_{P-C} = 2.7 Hz), 132.4 (d, J_{P-C} = 10.6 Hz), 133.5 (d, J_{P-C} = 108.2 Hz), 136.5 (s), 138.3 (d, J_{P-C} = 7.3 Hz), 143.0 (s), 158.2 (d, J_{P-C} = 14.0 Hz). ^{31}P{^{1}H} NMR (162 MHz, $CDCl_3$): δ 13.25. HRMS (ESI): *m*/*z* calcd. for $C_{28}H_{26}O_3P$: 441.1614 ([*M*+H]$^+$), found: 441.1608.

***cis*-6ab-Me.** Mp (MP-S3): 129.5–135.0 °C (dec.). ^{1}H NMR (400 MHz, $CDCl_3$): δ 2.84 (s, 3H, CH_3), 3.65(s, 3H, OCH_3), 3.81 (s, 3H, OCH_3), 6.01–6.02 (m, 1H), 6.21–6.23 (m, 1H), 6.49–6.52 (m, 1H), 6.87–6.91 (m, 1H), 6.95–6.97 (m, 1H), 7.01–7.04 (m, 1H), 7.14–7.16 (m, 1H), 7.33–7.37 (m, 1H), 7.40–7.54 (m, 5H), 7.71–7.76 (m, 2H), 7.86–7.91 (m, 1H). ^{13}C{^{1}H} NMR (100 MHz, $CDCl_3$): δ 20.6 (s, CH_3), 41.0 (d, J_{P-C} = 8.4 Hz, Ar_3C), 55.70 (s, OCH_3), 55.72 (s, OCH_3), 113.9 (d, J_{P-C} = 7.4 Hz), 114.1 (d, J_{P-C} = 2.4 Hz), 121.0 (d, J_{P-C} = 2.3 Hz), 123.3 (d, J_{P-C} = 5.9 Hz), 125.89 (s), 125.9 (s), 126.7 (d, J_{P-C} = 101.4 Hz), 128.58 (s), 128.63 (s), 128.7 (s), 128.8 (s), 129.7 (d, J_{P-C} = 101.2 Hz), 130.8 (s), 131.7 (d, J_{P-C} = 2.6 Hz), 131.9 (d, J_{P-C} = 9.9 Hz), 133.8 (d, J_{P-C} = 9.2 Hz), 135.5 (s), 136.2 (d, J_{P-C} = 108.0 Hz), 138.4 (d, J_{P-C} = 8.5 Hz), 143.8 (d, J_{P-C} = 1.4 Hz), 156.7 (d, J_{P-C} = 13.7 Hz), 158.3 (d, J_{P-C} = 13.3 Hz). ^{31}P{^{1}H} NMR (162 MHz, $CDCl_3$): δ 11.19. HRMS (ESI): *m*/*z* calcd. for $C_{28}H_{26}O_3P$: 441.1614 ([*M*+H]$^+$); found. 441.1605.

***trans*-6ab-Me.** Mp (MP-S3): 261.0–265.0 °C. ^{1}H NMR (400 MHz, $CDCl_3$): δ 2.91 (s, 3H, CH_3), 3.66 (s, 3H, OCH_3), 3.79 (s, 3H, OCH_3), 6.15 (d, $^4J_{P-H}$ = 1.4 Hz, 1H, $HCAr_3$), 6.90–7.04 (m, 5H), 7.14–7.18 (m, 2H), 7.23–7.28 (m, 1H), 7.32–7.36 (m, 1H), 7.43–7.52 (m, 4H), 7.70–7.75 (m, 2H). ^{13}C{^{1}H} NMR (151 MHz, $CDCl_3$): δ 20.5 (s), 40.8 (d, J_{P-C} = 8 Hz), 55.6 (d, J_{P-C} = 19 Hz), 113.6 (d, J_{P-C} = 2 Hz), 114.9 (d, J_{P-C} = 10 Hz), 120.1 (d, J_{P-C} = 2 Hz), 124.0 (d, J_{P-C} = 8 Hz), 125.9 (s), 127.0 (s), 128.3 (d, J_{P-C} = 14 Hz), 128.2 (d, J_{P-C} = 102 Hz), 128.4 (d, J_{P-C} = 12 Hz), 129.9 (d, J_{P-C} = 103 Hz), 130.0 (s), 130.5 (s), 130.8 (d, J_{P-C} = 11 Hz), 131.8 (d, J_{P-C} = 3 Hz), 132.4 (d, J_{P-C} = 10 Hz), 133.8 (d, J_{P-C} = 109 Hz), 134.7 (s), 135.3 (d, J_{P-C} = 8.3 Hz), 139.9 (d, J_{P-C} = 7 Hz), 142.4 (d, J_{P-C} = 2 Hz), 156.6 (s), 157.9 (s). ^{31}P{^{1}H} NMR (162 MHz, $CDCl_3$): δ 14.36. HRMS (ESI): *m*/*z* calcd. for $C_{28}H_{26}O_3P$: 441.1614 ([*M*+H]$^+$); found. 441.1611.

Determination of the Ratio of Isomers Obtained by the Friedel–Crafts Cyclizations. The ratios of the four isomers *cis*- and *trans*-**6aa** as well as *cis*- and *trans*-**6ab** in the reaction mixtures were estimated based on the integral ratio in the ^{31}P{^{1}H} NMR spectra. The reactions were conducted

essentially in the same manner with the experiments described above using **2a** and arylmagnesium bromides. The signals in the $^{31}P\{^{1}H\}$ NMR spectrum of the obtained mixture for the *o*-tolyl-substituted derivatives were identified based on the data for the purely isolated compounds, *cis*- and *trans*-**6aa-Me** as well as *cis*- and *trans*-**6ab-Me**, which are described previously (Fig. S31). In the case of the 2,6-dimethylphenyl-substituted derivatives, *i.e.*, *cis*- and *trans*-**6aa-Me$_2$** and *cis*- and *trans*-**6ab-Me$_2$**, however, all attempts to fully separate the isomers were unsuccessful. Therefore, we assigned the ^{31}P NMR signals based on the ^{31}P NMR chemical shifts of the isolated *trans*-**6aa-Me$_2$** and the experimental results including the R_f values for the *o*-tolyl series (Fig. S32). The observed NMR ratio of *trans*-**6aa-Me$_2$** of 30% seems consistent with the isolated yield of *trans*-**6aa-Me$_2$** (23% yield). The results thus obtained are summarized in Table S1. These results imply that the regioselectivity in the Friedel–Crafts cyclization is likely dependent on the bulkiness of the aryl groups at the benzyl position, *i.e.*, the less bulkier *o*-tolyl-substituted **3a-Me** gave a higher selectivity compared to **3a-Me$_2$**, although the reason remained unclear.

Table S1. Isomer Ratios of the Products Obtained by the Friedel–Crafts Cyclization

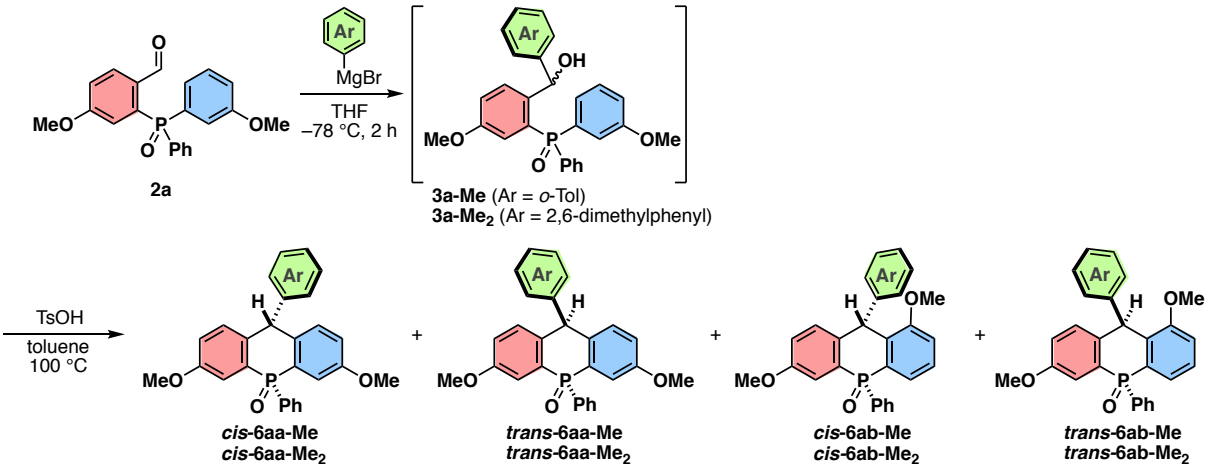

	Ratio / %[a]			
Substrate	*cis*-**6aa**	*trans*-**6aa**	*cis*-**6ab**	*trans*-**6ab**
3a-Me	10	59	15	16
	(6)[b]	(41)[b]	(10)[b]	(13)[b]
3a-Me$_2$	13	30	24	33

[a]Ratio estimated by the integral ratio of the signals in $^{31}P\{^{1}H\}$ NMR spectrum of the reaction mixture. [b]Isolated yield.

Synthesis of POF-Me from *trans*-6aa-Me. A solution of *trans*-**6aa-Me** (41.8 mg, 94.9 μmol) and NaO*t*-Bu (27.9 mg, 0.290 mmol) in DMSO (20 mL) was stirred at the ambient temperature for 16 h under an O_2 atmosphere. Then, 1*N* HCl aqueous solution (15 mL) was added, and the organic layer was separated. The aqueous layer was extracted with ethyl acetate three times. The combined organic layer was washed with water, dried over anhydrous Na_2SO_4, filtered, and concentrated under reduced pressure to give crude product containing **7aa-Me**.

To a solution of crude **7aa-Me** in MeOH (0.5 mL) was added an aqueous solution of HBr (47–48 wt%, 5 mL) dropwise under a N_2 atmosphere, and the mixture was heated at 90 °C. After stirring for 4.5 h at the same temperature, the mixture was allowed to cool to ambient temperature. After addition of CH_2Cl_2, the organic layer was separated. The aqueous layer was extracted with CH_2Cl_2 three times. The combined organic layer was washed with water, dried over anhydrous Na_2SO_4, filtered, and concentrated under reduced pressure. The mixture was purified by recrystallization from toluene to give 24.3 mg of POF-Me (59.2 μmol, 62% yield) as red crystals. The ^{1}H NMR spectrum of the product thus obtained was identical with that reported in ref. 3.

Synthesis of POF-Me$_2$ from *trans*-6aa-Me$_2$. This compound was prepared in a similar manner as described for POF-Me using *trans*-**6aa-Me$_2$** (46.0 mg, 0.101 mmol) as a starting material. Purification by recrystallization from toluene afforded 39.2 mg of POF-Me$_2$ (92.4 μmol, 91% yield) as red crystals: Mp (MP-S3): >300 °C. ^{1}H NMR (400 MHz, methanol-d_4): δ 2.02 (s, 3H), 2.06 (s, 3H), 6.60–6.75 (br, 2H), 6.98 (dd, J = 9.4, 6.4 Hz, 2H), 7.25 (d, J = 8.0 Hz, 2H), 7.27 (d, J = 8.8 Hz, 2H), 7.38 (dd, J = 7.6, 7.6 Hz, 1H), 7.50–7.60 (m, 2H), 7.60–7.70 (m, 3H). ^{13}C{^{1}H} NMR (150 MHz, methanol-d_4): δ 19.8 (s, CH_3), 20.0 (s, CH_3), 129.0 (d, J_{P-C} = 5.7 Hz, CH), 130.4 (s, CH), 130.5 (d, J_{P-C} = 11.5 Hz, CH), 131.5 (d, J_{P-C} = 11.5 Hz, CH), 133.6 (d, J_{P-C} = 111.3 Hz, C), 134.3 (s, CH), 136.9 (s, C), 136.9 (s, C), 137.6 (s, C), 155.5 (d, J_{P-C} = 7.2 Hz, C). ^{31}P{^{1}H} NMR (162 MHz, methanol-d_4): δ 9.07. HRMS (ESI): *m*/*z* calcd. for $C_{27}H_{21}NaO_3P$: 447.1121 ([*M*+Na]$^+$); found. 447.1120.

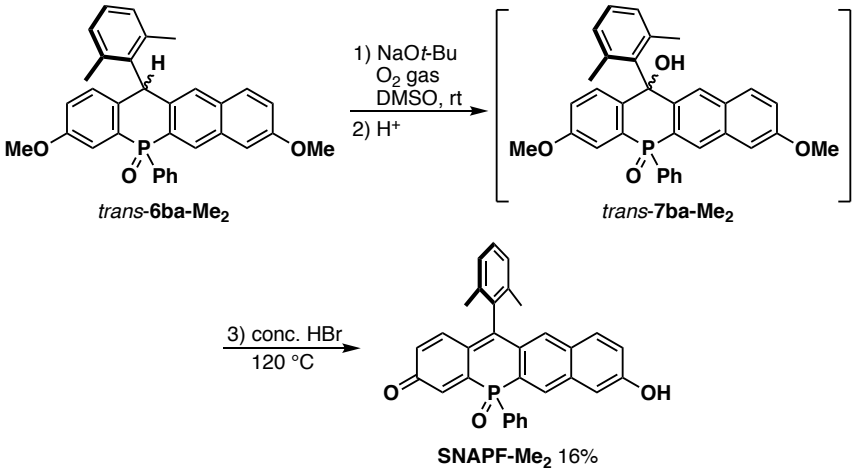

Scheme S4. Synthesis of seminaphtho-phospha-fluorescein SNAPF-Me$_2$.

Synthesis of SNAPF-Me$_2$ from *trans*-6ba-Me$_2$. This compound was prepared in a similar manner as described for POF-Me using *trans*-**6ba-Me$_2$** (68.3 mg, 0.135 mmol) as a starting material. The second-step reaction with HBr was conducted at 120 °C for 1 day. Purification by recrystallization from 1/1 CH_2Cl_2/MeOH afforded 10.0 mg of SNAPF-Me$_2$ (21.1 μmol, 16% yield) as deep red crystals. Mp (MP-S3): >300 °C. ^{1}H NMR (400 MHz, DMSO-d_6): δ 1.93 (s, 3H), 1.97 (s, 3H), 6.37 (dd, J = 10.0, 2.0 Hz, 1H), 6.84 (dd, J = 10.0, 6.4 Hz, 1H), 7.02 (dd, J = 16.4, 2.0 Hz, 1H), 7.18 (dd, J = 8.2, 2.4 Hz, 1H), 7.29–7.60 (m, 10H), 7.73 (d, J = 8.4 Hz, 1H), 8.52 (d, J = 14.8 Hz, 1H), 10.68 (s, 1H). ^{13}C{^{1}H} NMR (150 MHz, DMSO-d_6): δ 19.27 (s, CH_3), 19.30 (s, CH_3), 110.4 (s, C), 121.9 (s, CH), 125.4 (d, $J_{P–C}$ = 7.2 Hz, C), 126.4 (d, $J_{P–C}$ = 99.8 Hz, C), 127.8 (s, CH), 128.0 (s, CH), 128.5 (d, $J_{P–C}$ = 7.2 Hz, C), 128.6 (s, C), 129.0 (s, CH), 129.1 (s, CH), 129.1 (d, $J_{P–C}$ = 11.5 Hz, CH), 129.9 (d, $J_{P–C}$ = 10.1 Hz, CH), 132.2 (s, CH), 132.3 (s, CH), 132.8 (d, $J_{P–C}$ = 8.6 Hz, CH), 133.3 (d, $J_{P–C}$ = 5.7 Hz, CH), 133.8 (s, CH), 134.6 (d, $J_{P–C}$ = 107.1 Hz, C), 135.1 (s, C), 135.3 (s, C), 135.4 (d, $J_{P–C}$ = 21.6 Hz, C), 136.1 (s, C), 138.5 (d, $J_{P–C}$ = 8.8 Hz, CH), 140.4 (d, $J_{P–C}$ = 88.2 Hz, C), 152.2 (s, C), 159.6 (s, C), 183.1 (d, $J_{P–C}$ = 13.0 Hz, C). ^{31}P{^{1}H} NMR (162 MHz, DMSO-d_6): δ 6.3. HRMS (ESI): m/z calcd. for $C_{31}H_{23}NaO_3P$: 497.1277 ([M+Na]$^+$); found. 497.1283.

Structure of SNARF-Me$_2$ in Solution. We fully characterized the ^{1}H and ^{13}C NMR spectra of SNAPF-Me$_2$ based on the H–H COSY, HMBC, and HMQC techniques (Figs. S42–47). According to ^{1}H NMR (Fig. S42) and H–H COSY 2D NMR spectra (Fig. S45), the resonance signals at δ = 6.37 (dd, J = 10.0, 2.0 Hz, 1H), 6.84 (dd, J = 10.0, 6.4 Hz, 1H), 7.02 (dd, J = 16.4, 2.0 Hz, 1H) were unequivocally assigned to the protons H_A, H_B, and H_C, respectively, on the fused benzene moiety. Considering the fact that the proton B has a correlation with the ^{13}C resonance with δ of 183.1 (d, $^3J_{P–C}$ = 13.0 Hz, C) in the HMBC 2D-NMR spectrum (Fig. S46), this signal was assigned to the *C*=O moiety in a fused benzene ring. The chemical shift of 183.1 ppm corroborates that the C–O moiety on the fused benzene ring has significant character of C=O. Furthermore, in the HMBC spectrum, the pronounced correlations were observed between the phenolic proton (–O*H*) and the carbon atoms at 6 and 8 positions in the naphthalene moiety (i.e., the carbon atoms bearing H_D and H_E in Fig. S46). Based on these results, we concluded that the phenolic proton is localized on naphthol moiety, *i.e.*, the tautomer I is dominant even in solution.

2. X-ray Crystallographic Analysis

X-ray Data Collection of *trans*-6aa-Me. Colorless needle-shaped single crystals were grown by slow evaporation of a solution of *trans*-**6aa-Me** in CH_2Cl_2/hexane. Intensity data were collected at 123 K on a Rigaku Single Crystal X-ray diffractometer equipped with FR-X generator, Varimax optics, and PILATUS 200K photon counting detector with MoKα radiation (λ = 0.71075 Å). A total of 29556 reflections were measured with the maximum 2θ angle of 55.0°, of which 5130 were independent reflections (R_{int} = 0.0215). The structure was solved by direct methods (SIR-2003) and refined by the full-matrix least-squares on F^2 (SHELXL-2013). [1] All non-hydrogen atoms were refined anisotropically and all hydrogen atoms were placed using AFIX instructions. The crystal data are as

follows: $C_{28}H_{25}O_3P$; FW = 440.45, crystal size 0.20 × 0.07 × 0.05 mm^3, monoclinic, $P2_1/n$, a = 7.4318(16) Å, b = 19.171(4) Å, c = 15.802(4) Å, β = 94.986(3)°, V = 2242.8(9) Å^3, Z = 4, D_c = 1.304 g cm^{-3}, μ = 0.151 mm^{-1}, R_1 = 0.0377 ($I > 2\sigma(I)$), wR_2 = 0.975 (all data), GOF = 1.091. CCDC 1553532 contains the supplementary crystallographic data for this compound. This data can be obtained free of charge from The Cambridge Crystallographic Data Centre at www.ccdc.cam.ac.uk/data_request/cif.

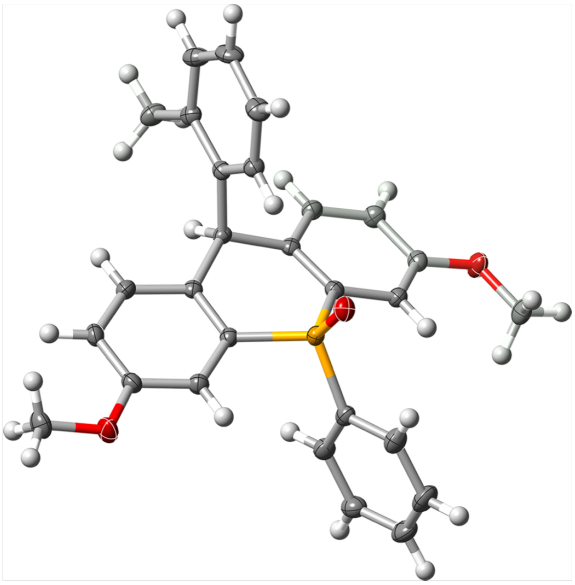

Fig. S1. Molecular structure of *trans*-**6aa-Me** (atomic displacement parameters set at 50% probability; only selected atoms are labelled; color scheme: grey, carbon; white, hydrogen; red, oxygen; orange, phosphorus).

X-ray Data Collection of *cis*-6ab-Me. Colorless platelet single crystals were grown by slow diffusion of pentane into a $CHCl_3$ solution of *cis*-**6ab-Me**. Intensity data were collected at 123 K on a Rigaku Single Crystal X-ray diffractometer equipped with FR-X generator, Varimax optics, and PILATUS 200K photon counting detector with MoKα radiation (λ = 0.71075 Å). A total of 24050 reflections were measured with the maximum 2θ angle of 55.0°, of which 4981 were independent reflections (R_{int} = 0.0773). The structure was solved by direct methods (SIR-2003) and refined by the full-matrix least-squares on F^2 (SHELXL-2013).[1] All non-hydrogen atoms were refined anisotropically and all hydrogen atoms were placed using AFIX instructions. The crystal data are as follows: $C_{28}H_{25}O_3P$; FW = 440.45, crystal size 0.17 × 0.09 × 0.04 mm^3, monoclinic, $P2_1/c$, a = 9.230(10) Å, b = 26.54(3) Å, c = 9.263(10) Å, β = 104.736(18)°, V = 2195(4) Å^3, Z = 4, D_c =1.333 g cm^{-3}, μ = 0.154 mm^{-1}, R_1 = 0.1174 ($I > 2\sigma(I)$), wR_2 = 0.3458 (all data), GOF = 1.056. CCDC 1553531 contains the supplementary crystallographic data for this compound. This data can be obtained free of charge from The Cambridge Crystallographic Data Centre at www.ccdc.cam.ac.uk/data_request/cif.

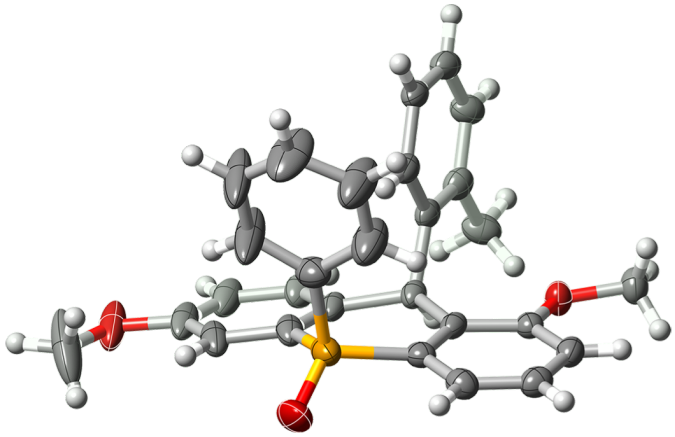

Fig. S2. Molecular structure of *cis*-**6ab-Me** (atomic displacement parameters set at 50% probability; only selected atoms are labelled; color scheme: grey, carbon; white, hydrogen; red, oxygen; orange, phosphorus).

X-ray Data Collection of SNAPF-Me$_2$. Deep-red block-shaped single crystals were grown by slow evaporation from a solution of SNAPF-Me$_2$ in 1/1 CH_2Cl_2/MeOH. Intensity data were collected at 123 K on a Rigaku Single Crystal X-ray diffractometer equipped with FR-X generator, Varimax optics, and PILATUS 200K photon counting detector with MoKα radiation (λ = 0.71075 Å). A total of 31735 reflections were measured with the maximum 2θ angle of 55.0°, of which 5501 were independent reflections (R_{int} = 0.0259). The structure was solved by direct methods (SIR-2003) and refined by the full-matrix least-squares on F^2 (SHELXL-2013).[1] All non-hydrogen atoms were refined anisotropically and all hydrogen atoms were placed using AFIX instructions. The crystal data are as follows: $C_{31}H_{23}O_3P$; FW = 474.46, crystal size 0.10 × 0.05 × 0.03 mm^3, monoclinic, $P2_1/n$, a = 9.7350(7) Å, b = 15.9966(9) Å, c = 15.9748(15) Å, β = 105.392(4)°, V = 2398.5(7) Å^3, Z = 4, D_c =1.314 g cm^{-3}, μ = 0.146 mm^{-1}, R_1 = 0.0348 ($I > 2\sigma(I)$), wR_2 = 0.0937 (all data), GOF = 1.063. CCDC 1553533 contains the supplementary crystallographic data for this compound. This data can be obtained free of charge from The Cambridge Crystallographic Data Centre at www.ccdc.cam.ac.uk/data_request/cif.

The Harmonic Oscillator Model of Aromaticity (HOMA) in SNAPF-Me$_2$. The harmonic oscillator model of aromaticity (HOMA)[2] were calculated for the X-ray crystal structure of SNAPF-Me$_2$ by using the following equation (eq.1):

$$\mathrm{HOMA} = 1 - \frac{\alpha}{n}\sum\left(R_{opt} - R_i\right)^2 \qquad \text{(eq. 1)}$$

Where α is an empirical normalization constant (α = 257.7 for C–C bonds)[2a], n is the number of C–C bonds taken into summation, R_{opt} is the optimal aromatic bond length (R_{opt} = 1.388 for C–C bonds)[2a], and R_i are the experimental bond lengths. The results were summarized in Fig. S3. HOMA of the ten-membered ring periphery of the naphthalene moiety (*i.e.*, the periphery of rings B and C) in

SNAPF provided values of 0.79, which is significantly larger than that of benzene moiety (ring A, –0.02). These results revealed that rings B and C in a naphthalene moiety retain strong aromatic character, whereas the ring A is nonaromatic.

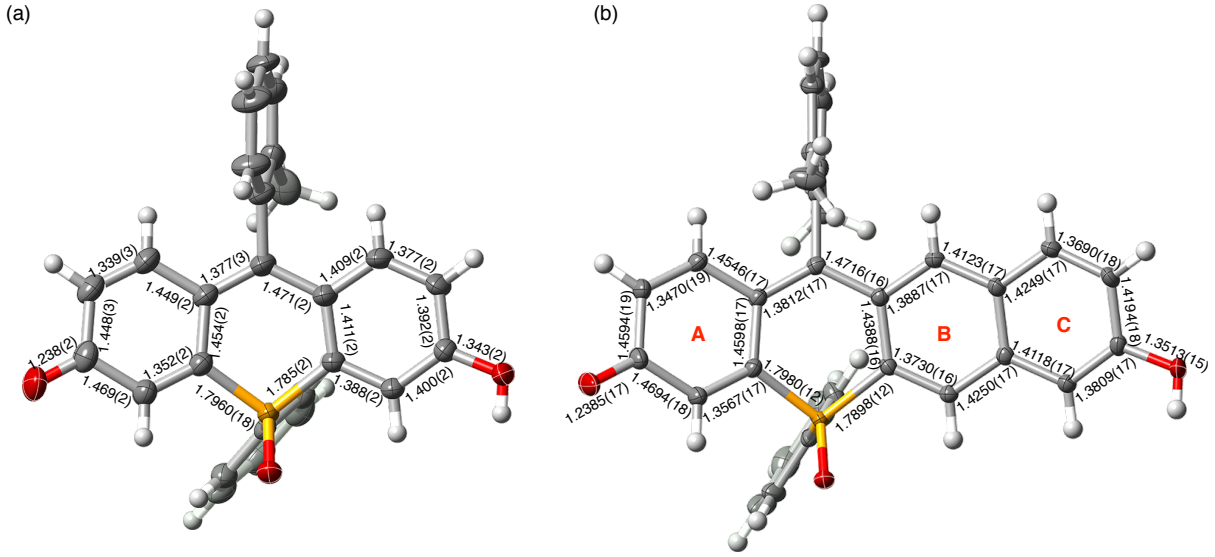

Fig. S3. Molecular structures and selected bond lengths (Å) of (a) POF-Me and (b) SNAPF-Me$_2$. Atomic displacement parameters set at 50% probability. Only selected atoms are labelled. Colour scheme: grey = carbon; white = hydrogen; red = oxygen; orange = phosphorus) and selected bond lengths (Å). The crystal structure of POF-Me has been reported in ref.3.

3. Computational Method and Results

Computational Method. All quantum chemical calculations were carried out using the GAUSSIAN 09 Revision E.01 suite of programs[4] with default thresholds and algorithms. The employed atomic basis sets was the 6-31+G(d) set.[5] Geometry optimizations of two tautomers **I** and **II** for charge-neutral SNAPF-Me, and the deprotonated forms of POF-Me, SNAPF-Me, and SNAF-Me in the ground state (S_0) were performed using density functional theory (DFT) with the B3LYP functional.[6] Stationary points in S_0 were optimized without any symmetry assumptions and characterized by frequency analysis at the same level of theory (the number of imaginary frequencies, NIMAG, was 0). The geometry optimizations of the deprotonated forms of POF-Me and SNAPF-Me in the lowest excited singlet state (S_1) were conducted using time-dependent DFT (TD-DFT) with the B3LYP functional. The Cartesian coordinates for the optimized geometries of these compounds are given in Tables S2–8. Frontier molecular orbitals of POF-Me, SNAPF-Me, and SNAF-Me are shown in Fig. S4. The molecular structures, the selected bond lengths, and the values of HOMA for these compounds are shown in Fig. S5–8. The values of HOMA were calculated based on the same procedure described in the section 2 (see p. S12).

Table S2. Cartesian Coordinates (Å) of the Optimized Structures for Tautomer **I** of Charge-neutral SNAPF-Me in S_0 (charge = 0)

atom	*x*	*y*	*z*
C	-5.51617846	-1.03790472	-0.56028248
H	-4.29905485	-2.65621558	-1.24708925
C	-4.30746926	-1.64852549	-0.84204342
C	-4.38221076	0.96128981	0.20969166
C	-3.09592295	-0.96279091	-0.60095958
C	-5.55371465	0.27802895	-0.02883789
C	-3.12135950	0.36613771	-0.06781966
C	-1.82417609	-1.54844935	-0.85823334
H	-6.51364392	0.74374530	0.18742991
H	-1.95757581	2.06529084	0.53651831
H	-4.41463548	1.97023922	0.61355976
C	-0.65152304	-0.86925294	-0.61945016
H	-1.78212608	-2.55936932	-1.25760677
C	-0.65998574	0.48449759	-0.12539129
C	-1.90407907	1.05200693	0.15237899
C	0.56345105	1.28653784	0.03140602
C	1.83066965	0.88676462	-0.36789120
P	0.89768623	-1.76993957	-0.91299926
C	2.12038096	-0.42038612	-0.96025674
C	3.33066243	-0.69800179	-1.51135398
H	3.52820651	-1.66099992	-1.97586848
C	2.95486785	1.81215034	-0.28696682
C	4.17242907	1.53647153	-0.81379169
H	2.79058263	2.76716738	0.20142964
H	4.99131698	2.24803786	-0.75463941
C	4.44328238	0.26867855	-1.50042920
C	0.38767464	2.66209435	0.61545858
C	0.04907244	5.18647795	1.79449310
C	0.17044271	3.78921466	-0.20821611
C	0.42835263	2.81510997	2.00890446
C	0.26404679	4.06847424	2.60213856
C	0.00351958	5.03911212	0.40636533
H	0.59535495	1.94003675	2.63272586
H	0.30401901	4.16696901	3.68371890
H	-0.16294374	5.91282226	-0.22002862
H	-0.08157423	6.16928146	2.24012192
C	0.13135345	3.67246793	-1.71558921
H	1.11360238	3.40303922	-2.12370041
H	-0.57275876	2.90042753	-2.04716373
H	-0.16903737	4.62126092	-2.17111252
O	-6.66124389	-1.74091823	-0.80857143
H	-7.43969845	-1.21218175	-0.57356372
O	5.53474184	0.01151705	-2.02046843
O	0.89470711	-2.68758147	-2.10429469
C	1.24664203	-2.69013376	0.63526288
C	1.82555580	-4.20947940	2.91642423
C	1.59731615	-4.04164722	0.51092249
C	1.18400524	-2.10390084	1.90856798
C	1.47317210	-2.86151101	3.04453141
C	1.88634834	-4.79760416	1.65072403
H	1.63733948	-4.48750049	-0.47891842
H	0.90896346	-1.05788847	2.01900654
H	1.42309867	-2.40187704	4.02842792
H	2.15862993	-5.84491247	1.54772309
H	2.05124577	-4.79798245	3.80215313

Table S3. Cartesian Coordinates (Å) of the Optimized Structures for Tautomer **II** of Charge-neutral SNAPF-Me in S_0 (charge = 0)

atom	*x*	*y*	*z*
C	-5.55904463	-1.32613792	-0.59903546
H	-4.16311869	-2.81839642	-1.36452099
C	-4.21986509	-1.83290939	-0.90914699
C	-4.50354753	0.72126463	0.29327130
C	-3.08749627	-1.10998102	-0.63565976
C	-5.62361796	0.00722776	0.02702326
C	-3.18488597	0.21059403	-0.02399728
C	-1.75952040	-1.61098145	-0.90944537
H	-6.61494184	0.38502683	0.26083528
H	-2.14823383	1.92159589	0.66643485
H	-4.56931304	1.70586114	0.75317109
C	-0.63531311	-0.88981654	-0.64185122
H	-1.66954222	-2.60648591	-1.33941934
C	-0.72040465	0.46730268	-0.10391846
C	-2.04740946	0.93624360	0.22227552
C	0.37955103	1.31138657	0.03674726
C	1.74369783	0.97376225	-0.38093554
P	0.96047989	-1.70825131	-0.91542417
C	2.11796278	-0.30370480	-0.88568551
C	3.40398266	-0.55021461	-1.35487403
H	3.66487068	-1.52313438	-1.76169153
C	2.75789649	1.96049311	-0.34338408
C	4.04735850	1.71343251	-0.79809807
H	2.52748310	2.94736629	0.04165786
H	4.79578913	2.50264762	-0.75506871
C	4.37659540	0.45594282	-1.31748058
C	0.16820787	2.68831810	0.60308994
C	-0.19065454	5.22701053	1.74690443
C	-0.17004257	3.78210976	-0.22539460
C	0.32347751	2.88331034	1.98341160
C	0.14427039	4.14275566	2.55954513
C	-0.34339628	5.03983572	0.37110684
H	0.58581630	2.03428911	2.61043245
H	0.26498970	4.27190456	3.63186674
H	-0.60541731	5.88707017	-0.25900670
H	-0.33322837	6.21420231	2.17892048
C	-0.35438805	3.61578011	-1.71727022
H	0.52927221	3.17015823	-2.18949940
H	-1.20190138	2.95863522	-1.94797135
H	-0.54068619	4.58206703	-2.19621279
O	-6.58217052	-1.98201038	-0.84466855
O	1.04662283	-2.58400541	-2.13553561
C	1.31541329	-2.66220087	0.61037800
C	1.87280906	-4.22811176	2.86495211
C	1.63305386	-4.01947306	0.46369893
C	1.27785997	-2.09262488	1.89243806
C	1.55543236	-2.87351906	3.01518453
C	1.91121825	-4.79897739	1.59057840
H	1.65731618	-4.45088009	-0.53308414
H	1.03025038	-1.04143941	2.01953786
H	1.52271719	-2.42759266	4.00607150
H	2.15653619	-5.85114592	1.47076757
H	2.08807481	-4.83525894	3.74061297
O	5.61502592	0.14767280	-1.79280177
H	6.20503844	0.91531822	-1.72499271

Table S4. Cartesian Coordinates (Å) of the Optimized Structures for the Deprotonated Form of POF-Me in S_0 (charge = –1)

atom	*x*	*y*	*z*
C	0.64858160	1.26716941	-0.27245424
C	1.23337716	-0.00020050	-0.00033187
C	0.64824066	-1.26740499	-0.27249052
C	-0.67086982	-1.42669746	-0.84234478
C	-0.67048024	1.42684569	-0.84230869

(Table S4 continued)

C	-1.15790215	2.65239981	-1.21681449
H	-2.14674084	2.74100586	-1.66057397
C	-1.15862428	-2.65210217	-1.21689899
C	-0.40051306	-3.89051076	-1.04342890
H	-2.14748192	-2.74042142	-1.66067279
C	-0.39943676	3.89058830	-1.04332886
P	-1.78693367	0.00023223	-1.00552629
C	1.38306138	-2.48691530	-0.06688564
C	0.90362778	-3.71870636	-0.42314122
H	2.37121935	-2.42418320	0.38029719
H	1.49450560	-4.61638120	-0.25570583
C	1.38374210	2.48646522	-0.06681494
C	0.90465030	3.71840128	-0.42303300
H	2.37188112	2.42344209	0.38037334
H	1.49577569	4.61590678	-0.25556319
O	-0.85091564	-5.00522269	-1.39331208
O	-0.84953633	5.00544086	-1.39315601
C	2.62388155	-0.00036965	0.58119032
C	5.18390635	-0.00061237	1.74492423
C	2.78284039	-0.00063419	1.97352658
C	3.76774418	-0.00020155	-0.24831645
C	5.03353980	-0.00033099	0.35565040
C	4.05091413	-0.00076489	2.56010544
H	1.89505262	-0.00075518	2.60144180
H	5.91764878	-0.00020721	-0.27949427
H	4.14903239	-0.00098227	3.64322024
H	6.17909986	-0.00070626	2.18409637
C	3.64066955	0.00018149	-1.75439581
H	4.62772608	-0.00013218	-2.22970455
H	3.09097566	0.88055438	-2.10793549
H	3.09021273	-0.87954401	-2.10833867
O	-2.69983256	0.00033053	-2.20592016
C	-2.78227937	0.00034351	0.54769971
C	-4.40396804	0.00037101	2.83711773
C	-4.17769801	-0.00008292	0.42503147
C	-2.20337236	0.00079743	1.82522686
C	-3.01050197	0.00081144	2.96442118
C	-4.98550911	-0.00007383	1.56656982
H	-4.61381884	-0.00038399	-0.57017064
H	-1.12160482	0.00115336	1.93130933
H	-2.55275274	0.00117776	3.95121833
H	-6.06833037	-0.00040065	1.46177228
H	-5.03184949	0.00038454	3.72557876

Table S5. Cartesian Coordinates (Å) of the Optimized Structures for the Deprotonated Form of SNAPF-Me in S_0 (charge = –1)

atom	*x*	*y*	*z*
H	-2.66923963	2.85686838	0.14652154
C	-2.87137896	1.88517266	-0.29470361
C	-3.38665643	-0.62062340	-1.42729551
C	-1.79115329	0.93273580	-0.37038617
C	-4.12752227	1.62825201	-0.76711686
C	-4.47413816	0.35761343	-1.38842876
C	-2.13569312	-0.35571960	-0.93693031
H	-4.91423378	2.37590516	-0.69866314
H	-3.61495556	-1.58934421	-1.86541791
C	0.68620936	0.46997379	-0.12598355
C	3.10140285	-1.05550262	-0.63033413
C	1.97692950	0.97466595	0.18551314
C	0.64418140	-0.87762006	-0.66257730
C	1.79273952	-1.58324632	-0.91090007
C	3.15163696	0.26969080	-0.04337113
H	2.06106737	1.97090849	0.61056103
P	-0.93357116	-1.72109282	-0.94555801
O	-0.99069976	-2.64967144	-2.13253026
O	-5.61185651	0.10959281	-1.84302617
C	-1.27385676	-2.65931340	0.60515935
C	-1.82240005	-4.19097164	2.89089334
C	-1.62019551	-4.01141129	0.48353929
C	-1.20153890	-2.07920219	1.88031176

(Table S5 continued)

C	-1.47490096	-2.84149914	3.01759773
C	-1.89394445	-4.77407096	1.62315506
H	-1.66864466	-4.45064623	-0.50911337
H	-0.92857143	-1.03246265	1.98753764
H	-1.41472020	-2.38372117	4.00243250
H	-2.16225313	-5.82308343	1.51907585
H	-2.03459779	-4.78393656	3.77783950
C	-0.47811919	1.28894182	0.02065362
C	-0.27403970	2.66881841	0.58956553
C	0.09719435	5.20983830	1.73541503
C	-0.37094075	2.85631929	1.97534647
C	0.01486396	3.77407297	-0.24213074
C	0.19533242	5.03112926	0.35312469
C	-0.18827388	4.11517170	2.55287586
H	-0.59402603	1.99853810	2.60543702
H	0.41812484	5.88541189	-0.28354961
H	-0.26778710	4.23563170	3.63068844
H	0.24302468	6.19724535	2.16760468
H	1.72196578	-2.58367402	-1.33347109
C	4.44574468	0.81247986	0.27011409
H	4.49064931	1.80843350	0.71119276
C	5.58995191	0.11381108	0.02522567
H	6.56714258	0.52816020	0.26324081
C	5.57911267	-1.22930856	-0.57179282
C	4.26873144	-1.76084755	-0.88010669
H	4.22721269	-2.75528136	-1.31936231
O	6.64507658	-1.85563675	-0.78871556
C	0.12883403	3.61822057	-1.74157045
H	0.92094834	2.90956345	-2.01122132
H	0.35512638	4.57871430	-2.21695195
H	-0.80150379	3.23345853	-2.17601035

Table S6. Cartesian Coordinates (Å) of the Optimized Structures for the Deprotonated Form of SNAF-Me in S_0 (charge = –1)

atom	*x*	*y*	*z*
C	-1.66990580	-2.06723022	-0.06755268
C	-4.37092574	-1.33110993	-0.12999365
C	-2.01057200	-0.66714998	-0.12482618
C	-2.61270688	-3.06024106	-0.04180622
C	-4.03185919	-2.75737567	-0.06918239
C	-3.41441804	-0.35919822	-0.15754314
H	-2.30724590	-4.10114864	0.00093094
H	-3.70462245	0.68750336	-0.20847674
H	-5.42883448	-1.08182278	-0.15571469
C	-0.98883264	0.29158695	-0.14061708
C	0.36696426	-0.11932636	-0.10522046
H	1.28464759	1.83430172	-0.15296543
C	1.47440983	0.76432513	-0.11124282
C	1.95001818	-2.00174434	-0.00988263
C	2.78732773	0.31900594	-0.06837785
C	0.66823333	-1.52613038	-0.05065559
C	3.07468711	-1.10948980	-0.01688330
C	3.90313300	1.22984478	-0.07424433
H	4.61008936	-2.61620780	0.06211127
H	2.11451546	-3.07518847	0.02934083
C	5.18733697	0.78215879	-0.03366744
H	3.68932738	2.29837725	-0.11314420
H	6.02861588	1.47202575	-0.03828115
C	5.51897215	-0.65232957	0.01873852
C	4.39258831	-1.55068112	0.02387523
O	-0.35252913	-2.44973655	-0.03656126
O	6.71711432	-1.03370982	0.05570219
O	-4.91695489	-3.64363574	-0.04410805
C	-1.32113322	1.75146791	-0.20210624
C	-1.93019542	4.48651291	-0.40140799
C	-1.38018935	2.38581700	-1.45111423
C	-1.56857937	2.49706604	0.97180068
C	-1.87044315	3.86099527	0.84645141
C	-1.68333916	3.74516118	-1.55812492
H	-1.18453001	1.79929540	-2.34546867

(Table S6 continued)

H	-2.06055208	4.44156304	1.74734974
H	-1.72394449	4.21764722	-2.53665747
H	-2.16647285	5.54625552	-0.46685895
C	-1.51129736	1.84915322	2.33669438
H	-2.27381034	1.06766936	2.44069158
H	-1.67316938	2.58995614	3.12724579
H	-0.54069740	1.36989896	2.51096762

Table S7. Cartesian Coordinates (Å) of the Optimized Structures for the Deprotonated Form of POF-Me in S_1 (charge = –1)

atom	*x*	*y*	*z*
C	0.72896914	1.25861941	-0.22625711
C	1.36185546	-0.00006835	0.01750480
C	0.72866152	-1.25857915	-0.22592749
C	-0.63249112	-1.40790765	-0.72706949
C	-0.63222551	1.40818962	-0.72710602
C	-1.16020116	2.66136194	-1.00192954
H	-2.16801915	2.75336821	-1.39911045
C	-1.16065339	-2.66100457	-1.00185499
C	-0.42479732	-3.88937454	-0.79105246
H	-2.16840246	-2.75285412	-1.39924630
C	-0.42400148	3.88959582	-0.79152084
P	-1.71858513	0.00023738	-1.00327976
C	1.45660228	-2.47762343	0.00031043
C	0.92973354	-3.71370341	-0.25927863
H	2.46954408	-2.40897393	0.38601973
H	1.50889062	-4.61750794	-0.08370697
C	1.45731860	2.47748763	-0.00058611
C	0.93067225	3.71367164	-0.26024432
H	2.47039609	2.40867148	0.38473327
H	1.51016045	4.61734964	-0.08511482
O	-0.88627896	-5.03146865	-1.03075264
O	-0.88531668	5.03176814	-1.03120684
C	2.77093174	-0.00014574	0.53638298
C	5.38834406	-0.00020814	1.57742929
C	3.00070015	0.00060576	1.92071550
C	3.87762715	-0.00090012	-0.34455605
C	5.17146598	-0.00092686	0.19694563
C	4.29550855	0.00057262	2.44598021
H	2.14397883	0.00121759	2.59060343
H	6.02429239	-0.00150612	-0.47987128
H	4.44578732	0.00114752	3.52323861
H	6.40348562	-0.00024637	1.96841264
C	3.67804805	-0.00163977	-1.84294992
H	4.64105109	-0.00183343	-2.36550795
H	3.11119625	0.87764673	-2.17186933
H	3.11130642	-0.88130776	-2.17104460
O	-2.50755536	0.00021552	-2.29493393
C	-2.94039839	0.00038382	0.39366772
C	-4.85467336	0.00005931	2.45104639
C	-4.30836592	-0.00077099	0.09014516
C	-2.54053662	0.00138146	1.73781674
C	-3.49015035	0.00122757	2.76177221
C	-5.26144648	-0.00094199	1.11393551
H	-4.60589226	-0.00145484	-0.95482848
H	-1.48117550	0.00229312	1.98595076
H	-3.16718137	0.00203700	3.80083804
H	-6.32122063	-0.00183355	0.86664015
H	-5.59519680	-0.00006558	3.24828982

Table S8. Cartesian Coordinates (Å) of the Optimized Structures for the Deprotonated Form of SNAPF-Me in S_1 (charge = –1)

atom	*x*	*y*	*z*
H	-2.62176588	2.85492654	0.15542615
C	-2.80485982	1.91984694	-0.36641453
C	-3.26886297	-0.54554331	-1.65490400
C	-1.71345591	0.95303911	-0.43718129
C	-4.01108184	1.70298654	-0.94725602
C	-4.31687585	0.46249468	-1.67751573
C	-2.04891288	-0.34133784	-1.05073081
H	-4.80304767	2.44685960	-0.89789144
H	-3.48964269	-1.49744974	-2.13152803
C	0.74429724	0.39986205	-0.16938751
C	3.10611642	-1.20138383	-0.63443998
C	2.02393085	0.91055801	0.05224972
C	0.65390589	-0.96504130	-0.61198511
C	1.79395882	-1.72165999	-0.83747497
C	3.20244880	0.15792527	-0.16322766
H	2.13966691	1.93529962	0.39346644
P	-0.94202208	-1.75765169	-0.88803449
O	-1.02146719	-2.76643617	-2.00864871
O	-5.41685629	0.29560650	-2.24653296
C	-1.39412820	-2.56439576	0.70707043
C	-2.23966975	-3.80896828	3.08432580
C	-2.29122569	-3.64564996	0.66650351
C	-0.92193505	-2.11919645	1.95217549
C	-1.33844787	-2.73973963	3.13232585
C	-2.71371318	-4.25961099	1.84724364
H	-2.63512913	-4.00923563	-0.29791423
H	-0.21443102	-1.29511387	1.99933226
H	-0.95430329	-2.39246823	4.08915744
H	-3.40614513	-5.09760580	1.80139415
H	-2.56497684	-4.29097438	4.00363764
C	-0.44525383	1.28689455	0.00650575
C	-0.20123981	2.62270987	0.64223206
C	0.26845701	5.08819840	1.91985454
C	-0.15191924	2.71616795	2.04235885
C	0.00394518	3.78787633	-0.13363069
C	0.23295406	5.00473918	0.52595733
C	0.07595233	3.93535012	2.68406768
H	-0.30307089	1.81441955	2.63106125
H	0.39023546	5.90262788	-0.06913668
H	0.10192906	3.98160161	3.77032438
H	0.44874351	6.04589637	2.40300841
H	1.68640175	-2.74374432	-1.19355518
C	4.50192215	0.71235129	0.06792758
H	4.56923816	1.74062605	0.42269967
C	5.63388167	-0.02302678	-0.15025293
H	6.62249399	0.39585033	0.02355600
C	5.58825214	-1.40941977	-0.62970259
C	4.27688659	-1.94850336	-0.85776776
H	4.20889347	-2.97264278	-1.21753605
O	6.65516788	-2.05974078	-0.82309322
C	-0.02461953	3.73698451	-1.64448667
H	0.62096234	2.94040557	-2.03152057
H	0.31060060	4.68811494	-2.07255514
H	-1.03532275	3.53490011	-2.02135000

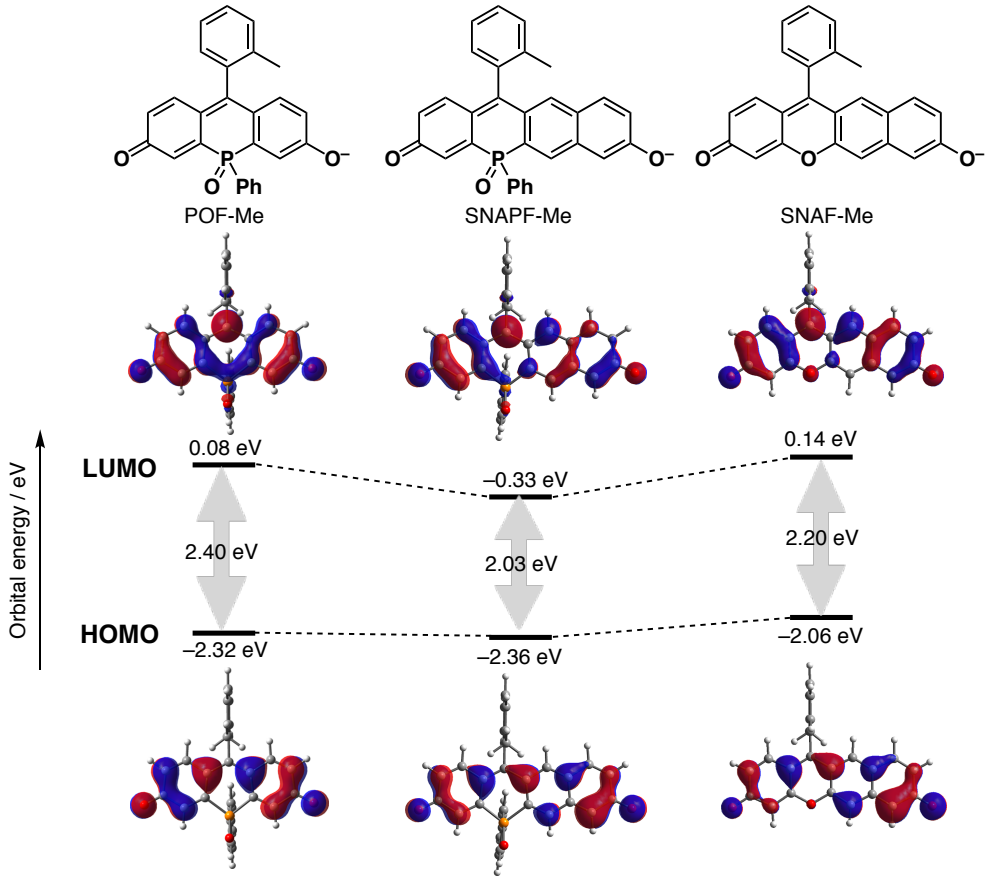

Fig. S4. Energy diagrams and pictorial representation of Kohn-Sham HOMOs and LUMOs for the deprotonated forms of POF-Me, SNAPF-Me, and SNAF-Me calculated at the B3LYP/6-31+G(d) level of theory (isovalue = 0.03).

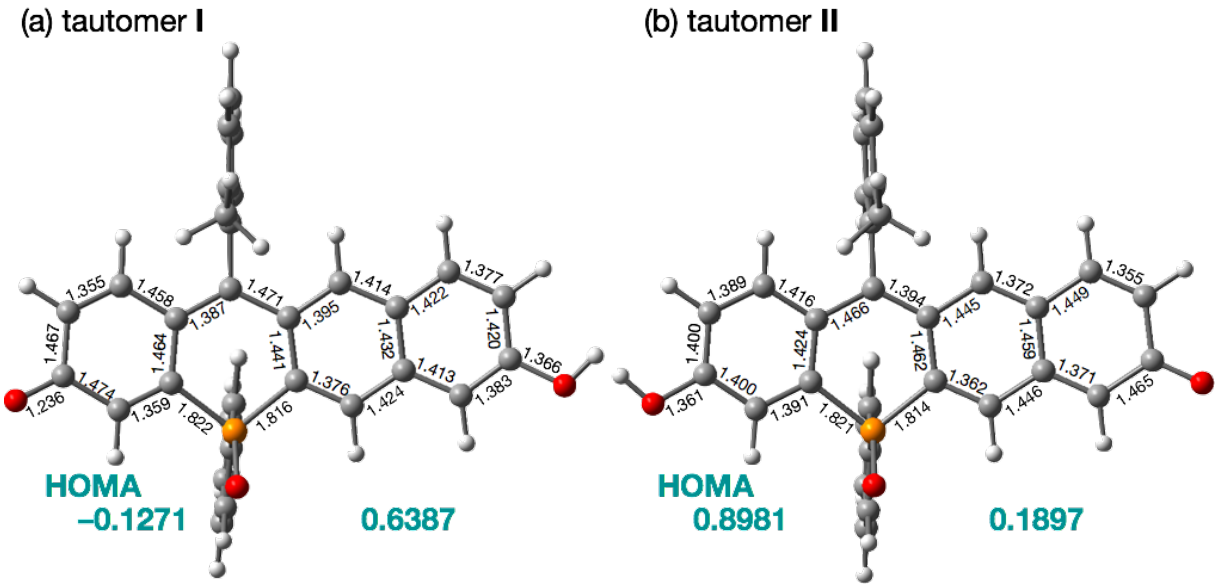

Fig. S5. Optimized geometries, the selected bond lengths (Å), and the HOMA values of the tautomers (a) **I** (b) and **II** of SNAPF-Me in S_0.

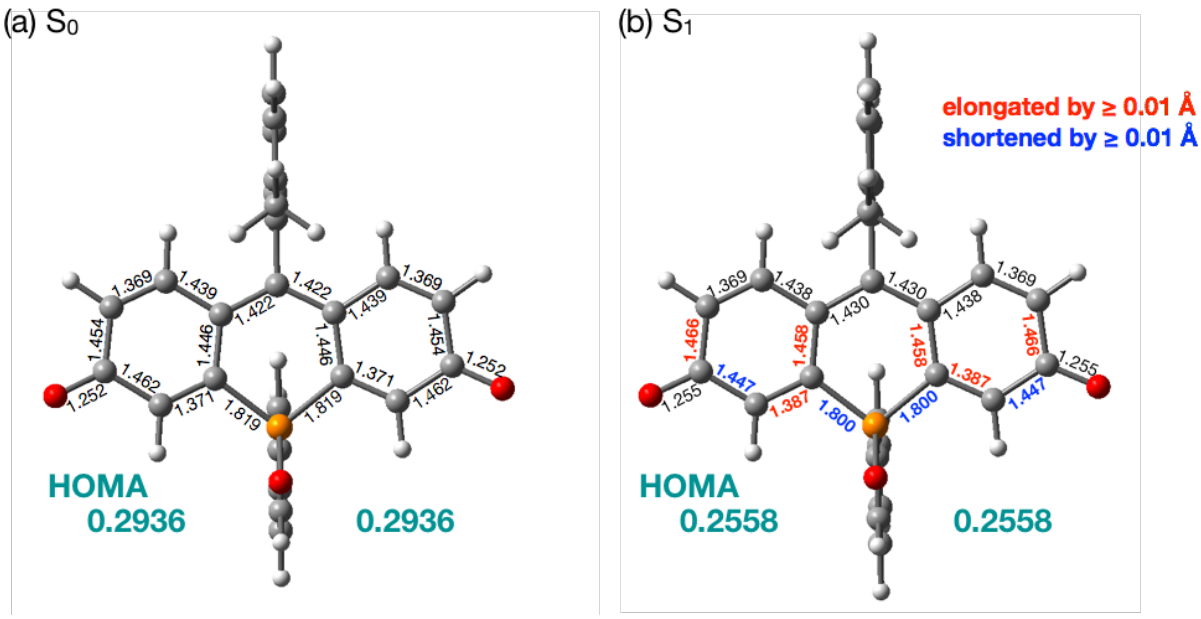

Fig. S6. Optimized geometries, the selected bond lengths (Å), and the HOMA values of the deprotonated form of POF-Me in (a) S_0 and (b) S_1.

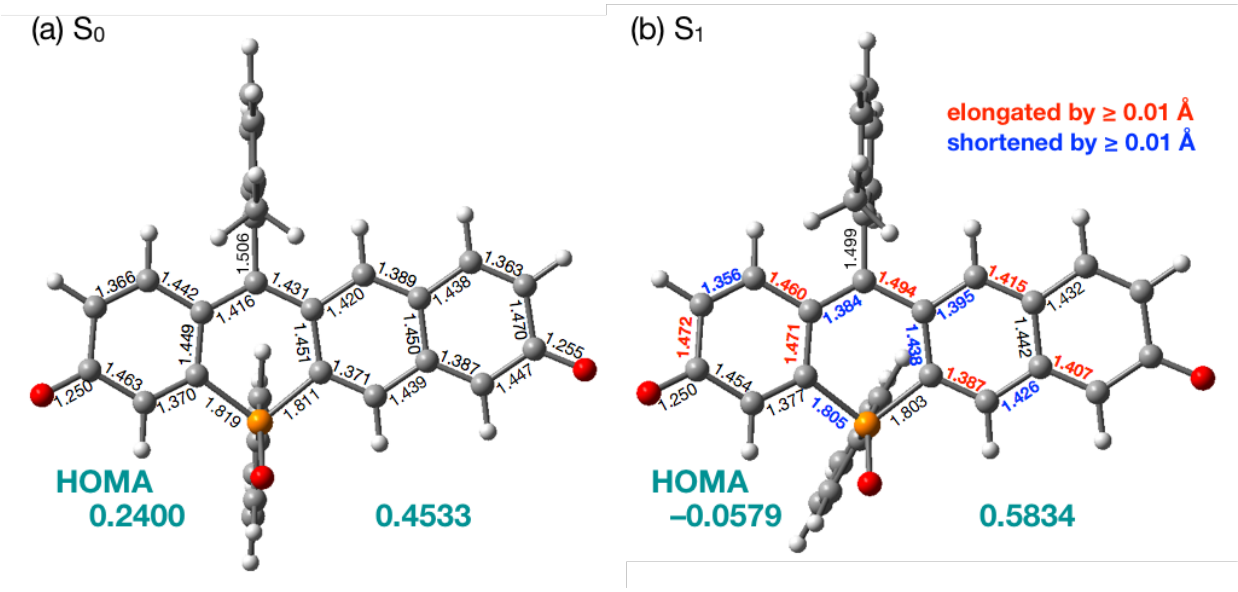

Fig. S7. Optimized geometries, the selected bond lengths (Å), and the HOMA values of the deprotonated form of SNAPF-Me in (a) S_0 and (b) S_1.

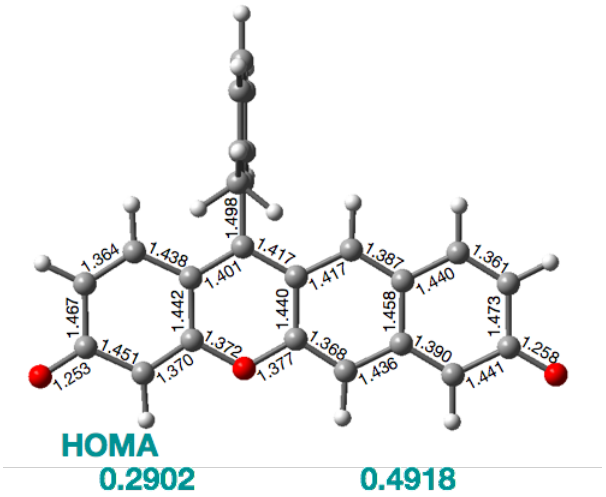

Fig. S8. Optimized geometry, the selected bond lengths (Å), and the HOMA values of the deprotonated form of SNAF-Me in S_0.

4. Photophysical Properties

Photophysical measurements. UV-vis-NIR absorption spectra of POF-Me_2 and SNAPF-Me_2 were measured with a Shimadzu UV-3600 Plus spectrometer with a resolution of 0.2 nm using 10^{-5} M sample solutions in aqueous buffer solutions (pH = 2: 10 mM KCl/HCl aqueous solution, pH = 3–7: citric acid/Na_2HPO_4 aqueous solutions, pH = 8: 10 mM tris(hydroxymethyl)aminomethane/HCl, pH = 9–11: Na_2CO_3/$NaHCO_3$ aqueous solutions) containing 1% DMSO in a 1 cm square quartz cuvette. Emission spectra were measured with a Horiba SPEX Fluorolog 3 spectrofluorometer equipped with a Hamamatsu PMA R5509-73 and a cooling system C9940-01 with a resolution of 1.0 nm using 10^{-6} M sample solutions. Absolute fluorescence quantum yields were determined with a Hamamatsu photonics PMA-11 calibrated integrating sphere system.

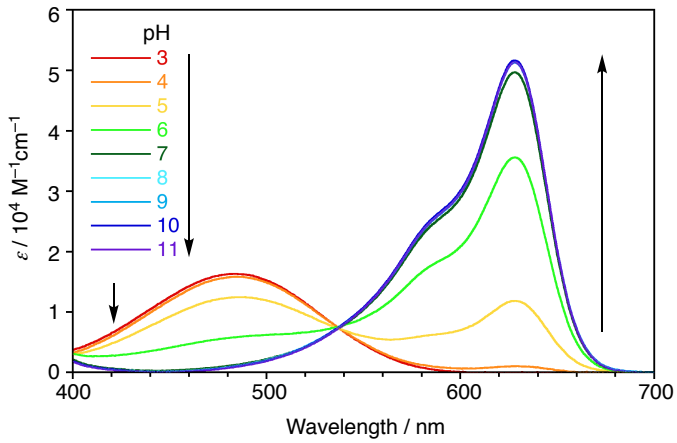

Fig. S9. Absorption spectra of POF-Me_2 in aqueous buffer solutions with various pH values containing 1% DMSO.

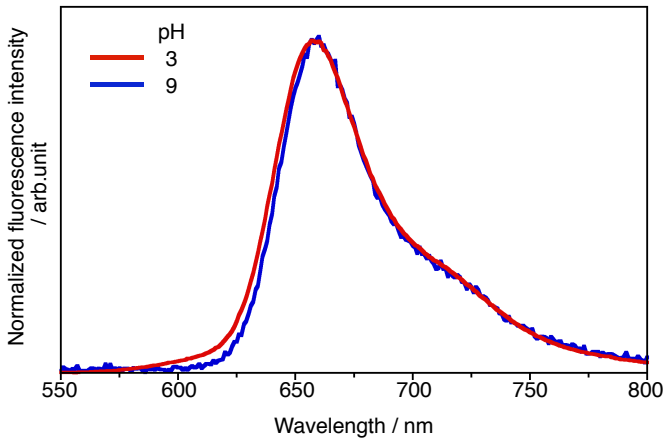

Fig. S10. Fluorescence spectra of POF-Me_2 excited at 500 nm in pH-buffer solutions (pH = 3: 50 mM citric acid/sodium citrate, pH = 9: 100 mM Na_2CO_2/$NaHCO_3$) containing 1% DMSO.

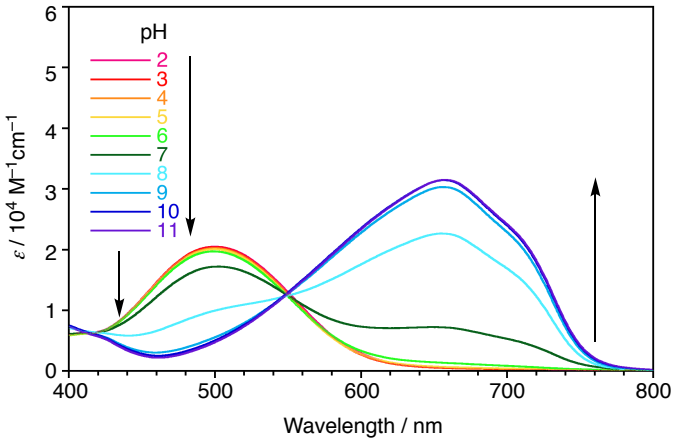

Fig. S11. Absorption spectra of SNAPF-Me_2 in aqueous buffer solutions with various pH values containing 1% DMSO.

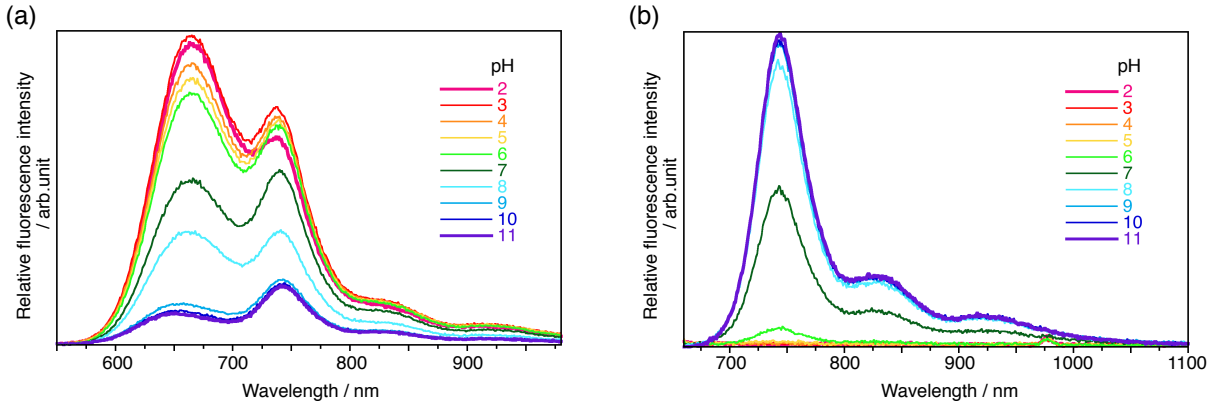

Fig. S12. Fluorescence spectra of SNAPF-Me_2 excited at (a) 500 nm and (b) 650 nm in aqueous buffer solutions with various pH values containing 1% DMSO.

Dual Emission of SNAPF under the Acidic Conditions. Upon excitation at 500 nm, SNAPF-Me_2 showed another shorter-wavelength emission band at λ_{em} = 655 nm (Fig. S12a). The ratio of fluorescence intensities of the two emission bands (I_{655}/I_{744}) changes from 1.41/1 (pH = 2) to 0.64/1 (pH = 11) upon increasing pH values. Considering this pH dependence, the emission bands at λ_{em} = 655 nm and λ_{em} = 744 nm are assigned to the emission from the charge-neutral and deprotonated SNAPF-Me_2, respectively. Whereas similar dual-fluorescence behavior has already been observed in POFs under the acidic conditions, the ratio of fluorescence intensities of the two emission bands (I_{655}/I_{744}) in SNAPF-Me_2 of 1.27/1 at pH = 3 is much larger than those (I_{600}/I_{656}) in POF-Me (1/15) and POF-Me_2 (1/60). The high ratio values for POF-Me and POF-Me_2 even under the acidic conditions can be explained by the higher pK_a values in the excited state, which result in the deprotonation in the excited state. In contrast, the low I_{655}/I_{744} ratio values of SNAPF under the acidic conditions suggest that the pK_a value of this compound retains higher in the excited state compared to those of POFs, and the excited-state proton transfer process is suppressed, although other possibility, such as lower Φ_{FL} of the longer-wavelength emission bands, cannot be excluded.

Determination of pK_a Values. Relative absorbances of POF-Me_2 and SNAPF-Me_2 at the maximum wavelengths of the longest absorption bands A_x (where x = 628 nm and 654 nm for POF-Me_2 and SNAPF-Me_2, respectively) at various pH values were plotted against the pH values (Fig. S13), and were analyzed by non-linear least square curve fitting using the following equation (eq. 2):

$$A_x = \frac{10^{-\mathrm{pH}}A_0 + 10^{-\mathrm{p}Ka}A_\infty}{10^{-\mathrm{pH}} + 10^{-\mathrm{p}Ka}} \qquad \text{(eq. 2)}$$

where A_0 and A_∞ represent the initial and final absorbance values, respectively.

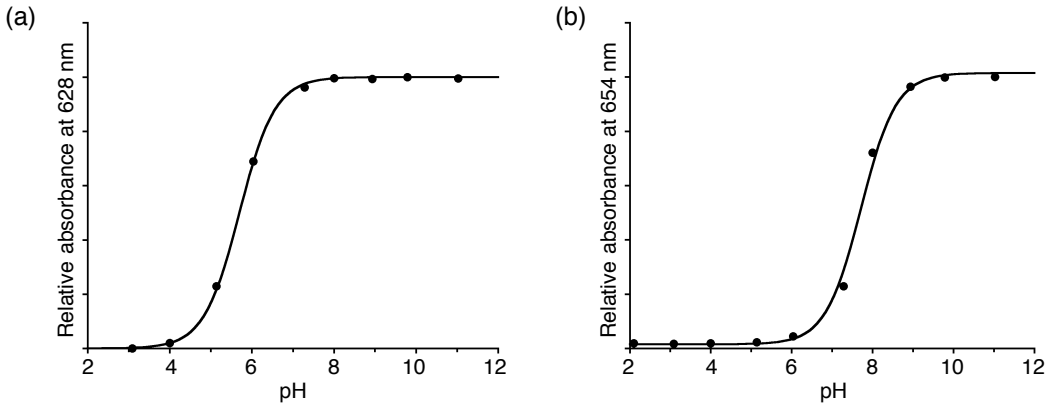

Fig. S13. Plots of relative absorbance of (a) POF-Me_2 at 628 nm (A_{627}) and (b) SNAPF-Me_2 at 654 nm (A_{654}) as a function of the pH value and their fitting curves (R^2 = 0.99971 and 0.99695 for POF-Me_2 and SNAPF-Me_2, respectively).

5. References

1 G. M. Sheldrick, *SHELX-2013, Program for the Refinement of Crystal Structures*; University of Gottingen: Gottingen, Germany, 2013.

2 (a) J. Kruszewski and T. M. Krygowski, *Tetrahedron Lett.*, 1972, **13**, 3839. (b) T. M. Krygowski, *J. Chem. Inf. Model.*, 1993, **33,** 70. (c) T. M. Krygowski and M. K. Cyra´nski, *Chem. Rev.*, 2001, **101**, 1385.

3 A. Fukazawa, S. Suda, M. Taki, E. Yamaguchi, M. Grzybowski, Y. Sato, T. Higashiyama and S. Yamaguchi, *Chem*. *Commun*., 2016, **52**, 1120.

4 Gaussian 09, Revision C.01, M. J. Frisch, G. W. Trucks, H. B. Schlegel, G. E. Scuseria, M. A. Robb, J. R. Cheeseman, G. Scalmani, V. Barone, B. Mennucci, G. A. Petersson, H. Nakatsuji, M. Caricato, X. Li, H. P. Hratchian, A. F. Izmaylov, J. Bloino, G. Zheng, J. L. Sonnenberg, M. Hada, M. Ehara, K. Toyota, R. Fukuda, J. Hasegawa, M. Ishida, T. Nakajima, Y. Honda, O. Kitao, H. Nakai, T. Vreven, J. A. Montgomery, Jr., J. E. Peralta, F. Ogliaro, M. Bearpark, J. J. Heyd, E. Brothers, K. N. Kudin, V. N. Staroverov, T. Keith, R. Kobayashi, J. Normand, K. Raghavachari, A. Rendell, J. C. Burant, S. S. Iyengar, J. Tomasi, M. Cossi, N. Rega, J. M. Millam, M. Klene, J. E. Knox, J. B. Cross, V. Bakken, C. Adamo, J. Jaramillo, R. Gomperts, R. E. Stratmann, O. Yazyev, A. J. Austin, R. Cammi, P–Comelli, J. W. Ochterski, R. L. Martin, K. Morokuma, V. G. Zakrzewski, G. A. Voth, P. Salvador, J. J. Dannenberg, S. Dapprich, A. D. Daniels, O. Farkas, J. B. Foresman, J. V. Ortiz, J. Cioslowski, D. J. Fox, Gaussian, Inc., Wallingford CT, 2010.

5 (a) R. Ditchfield, W. J. Hehre, J. A. Pople, *J. Chem*. *Phys*., 1971, **54**, 724–728. (b) W. J. Hehre, R. Ditchfield, J. A. Pople, *J. Chem*. *Phys*., 1972, **56**, 2257–2261. (c) P. C. Hariharan, J. A. Pople, *Theor*. *Chim*. *Acta*, 1973, **28**, 213–222. (d) M. M. Francl, W. J. Pietro, W. J. Hehre, J. S. Binkley, M. S. Gordon, D. J. DeFrees, J. A. Pople, *J. Chem. Phys.*, 1982, **77**, 3654–3665.

6 (a) A. D. Becke, *Phys. Rev. A*, 1988, **38**, 3098–3100. (b) C. Lee, W. Yang, R. G. Parr, *Phys. Rev. B*, 1988, **37**, 785–789. (c) A. D. Becke, *J. Chem. Phys.*, 1993, **98**, 5648–5652.

6. NMR Spectra

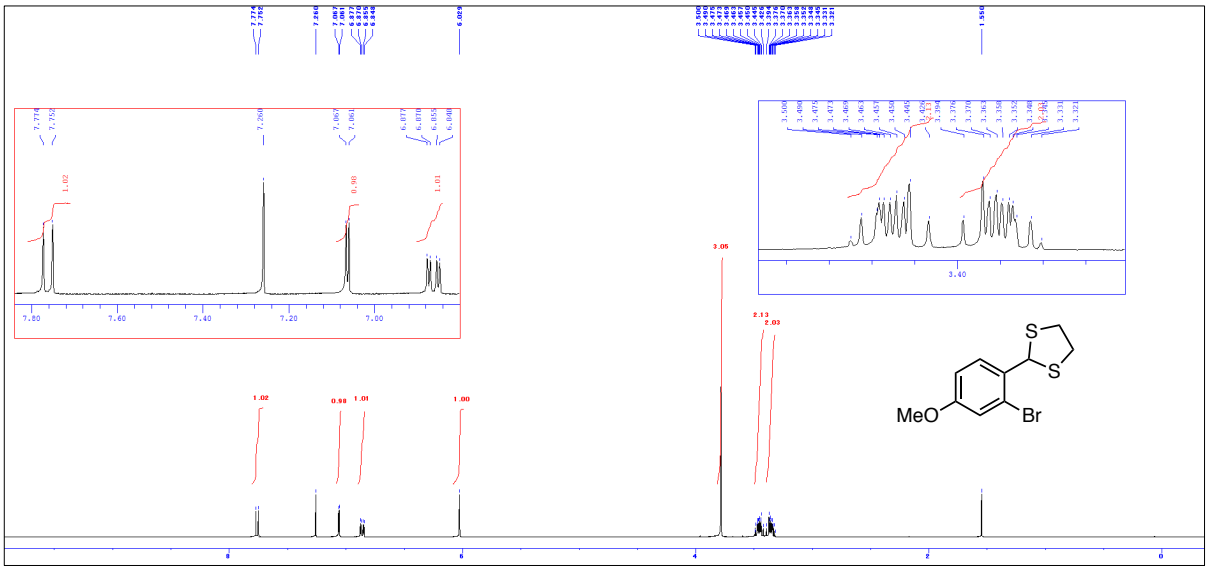

Fig. S14. ^{1}H NMR spectrum of **8** (400 MHz, $CDCl_3$).

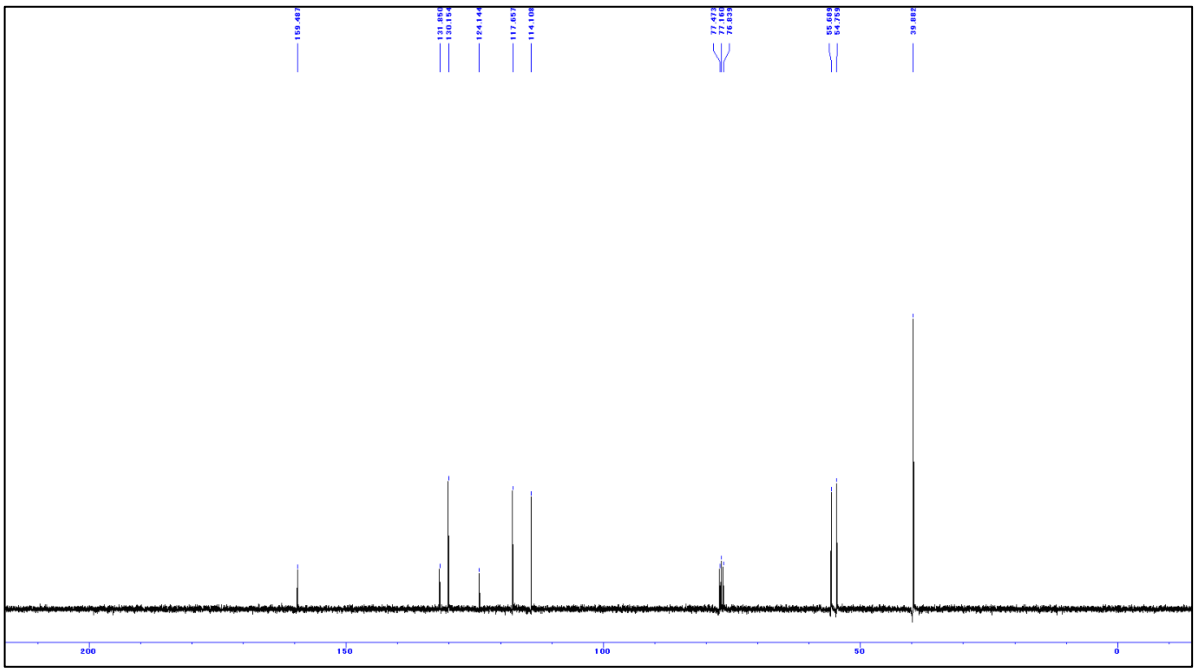

Fig. S15. $^{13}C\{^{1}H\}$ NMR spectrum of **8** (100 MHz, $CDCl_3$).

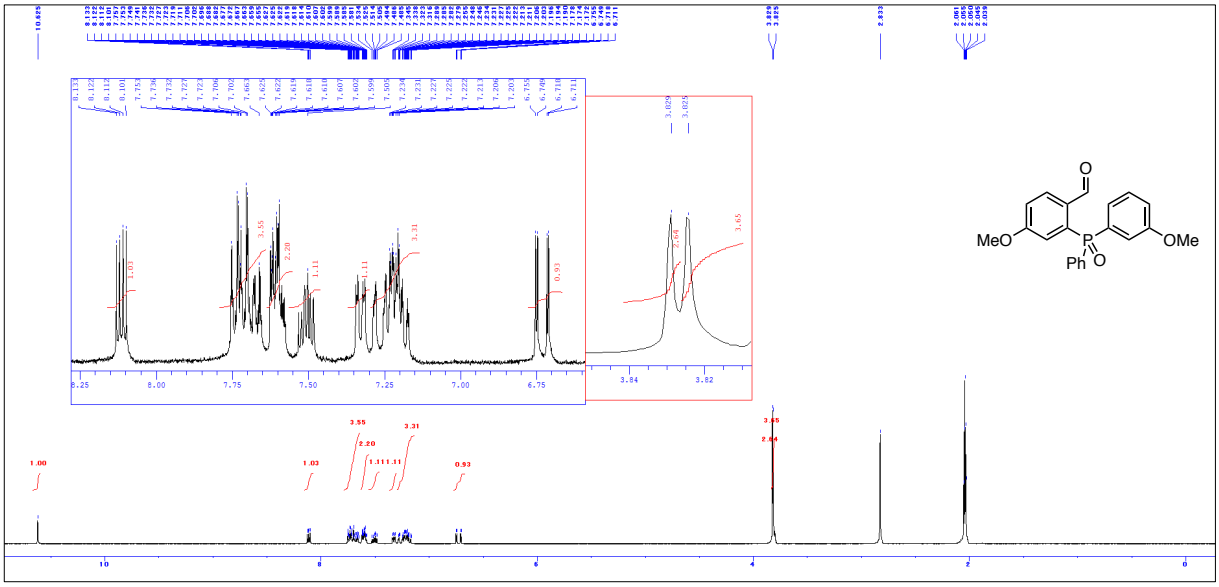

Fig. S16. ^{1}H NMR spectrum of **2a** (400 MHz, acetone-d_6).

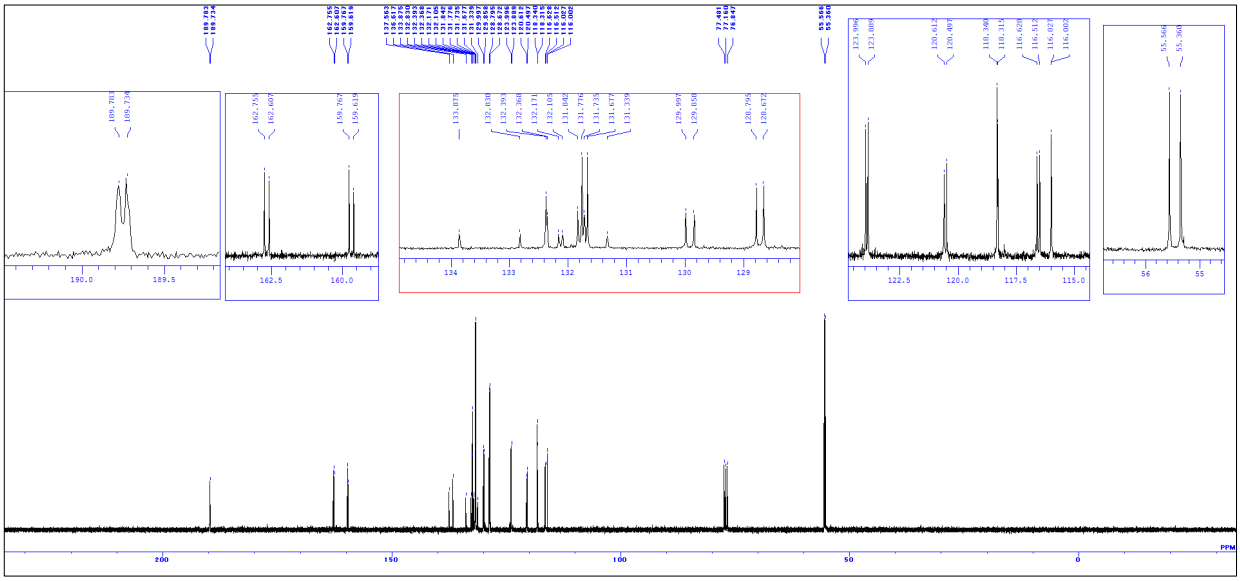

Fig. S17. $^{13}C\{^{1}H\}$ NMR spectrum of **2a** (100 MHz, $CDCl_3$).

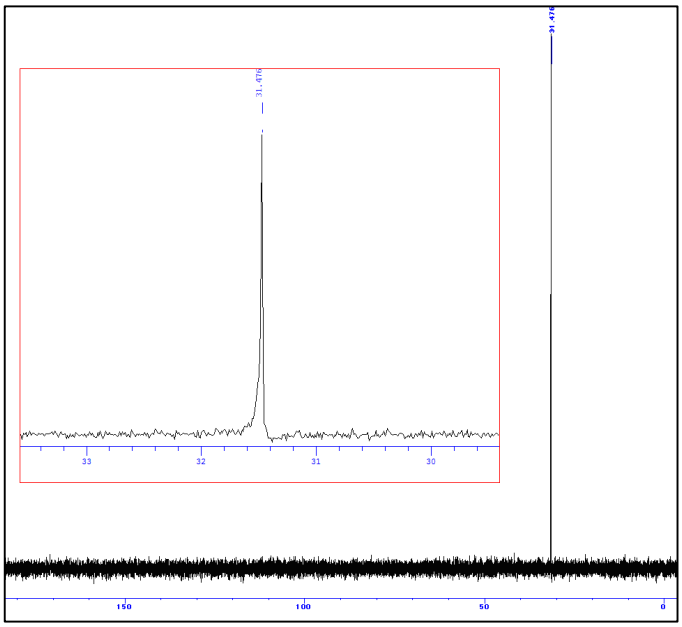

Fig. S18. $^{31}P\{^{1}H\}$ NMR spectrum of **2a** (162 MHz, $CDCl_3$).

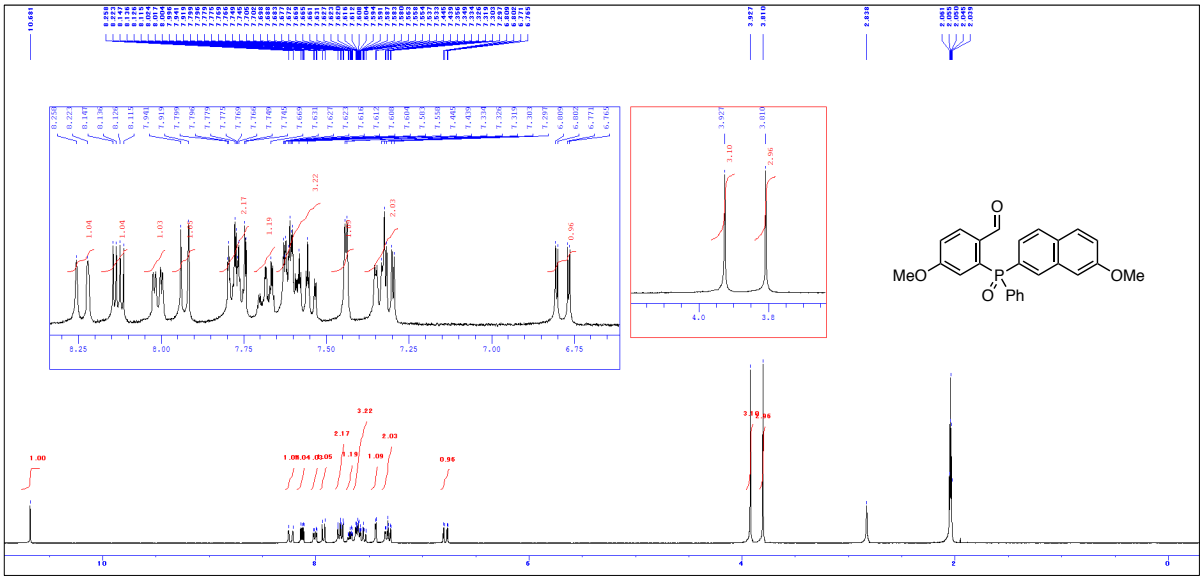

Fig. S19. ^{1}H NMR spectrum of **2b** (400 MHz, acetone-d_6).

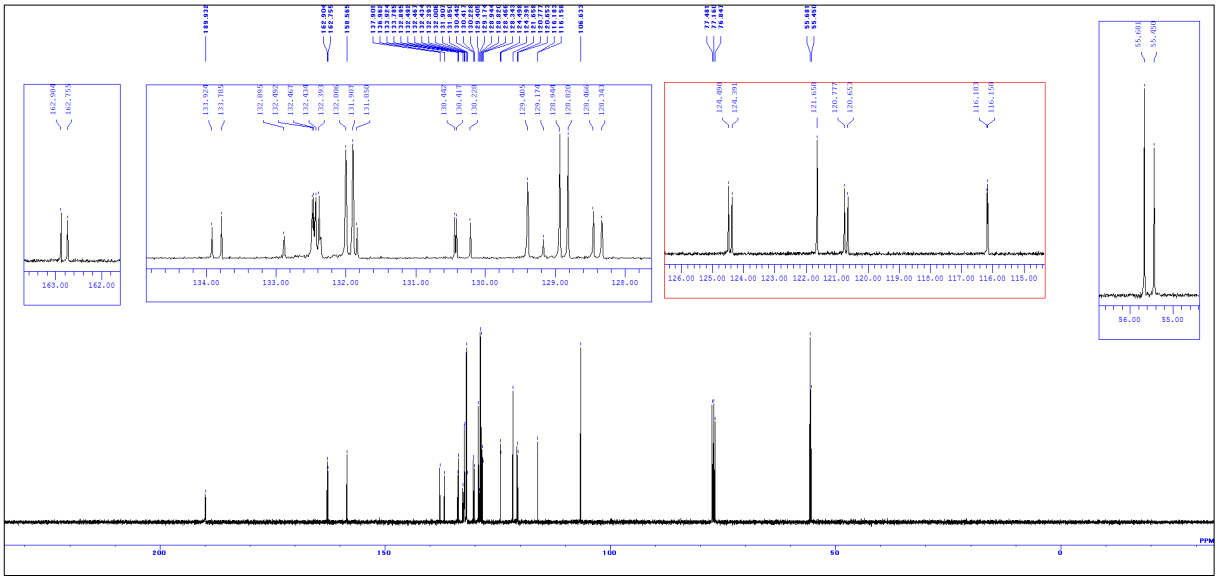

Fig. S20. $^{13}C\{^{1}H\}$ NMR spectrum of **2b** (100 MHz, $CDCl_3$).

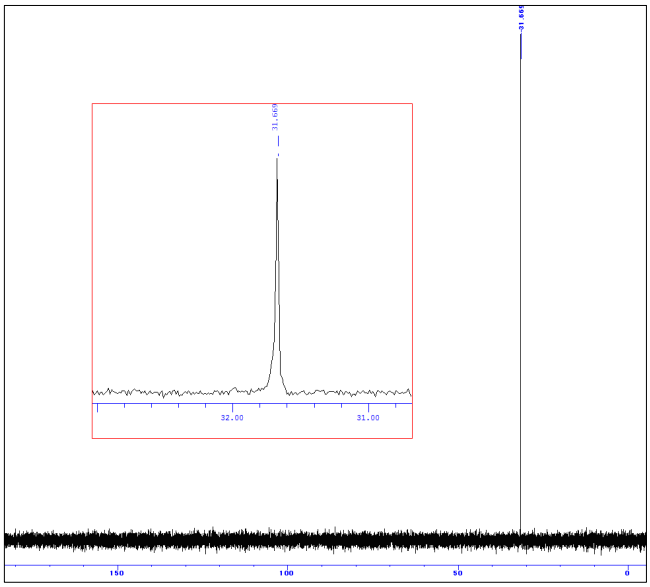

Fig. S21. $^{31}P\{^{1}H\}$ NMR spectrum of **2b** (162 MHz, $CDCl_3$).

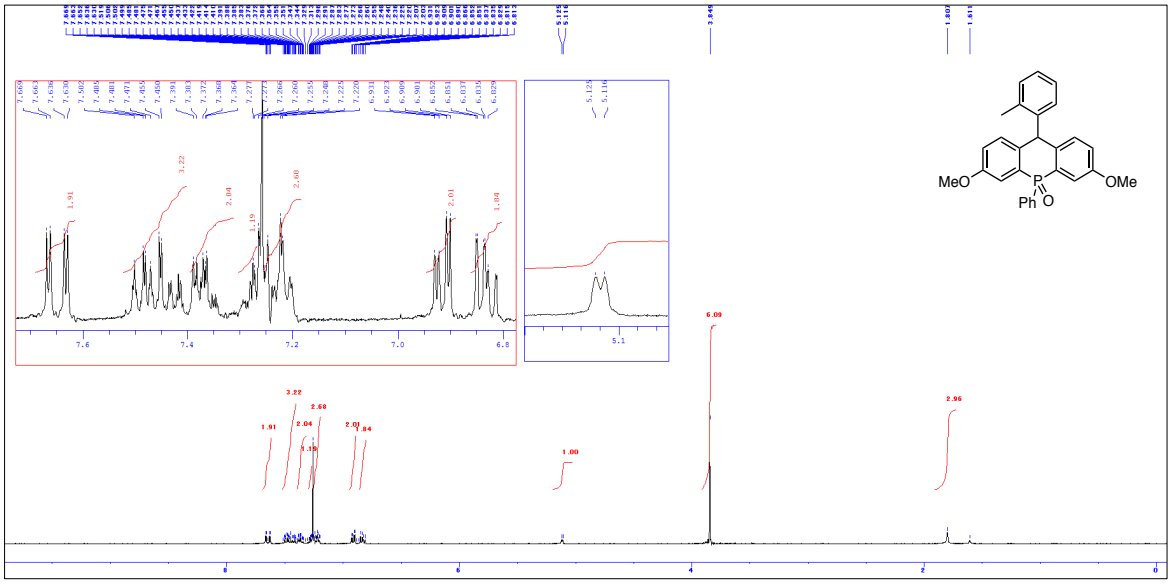

Fig. S22. ^{1}H NMR spectrum of *trans*-**6aa-Me** (400 MHz, $CDCl_3$).

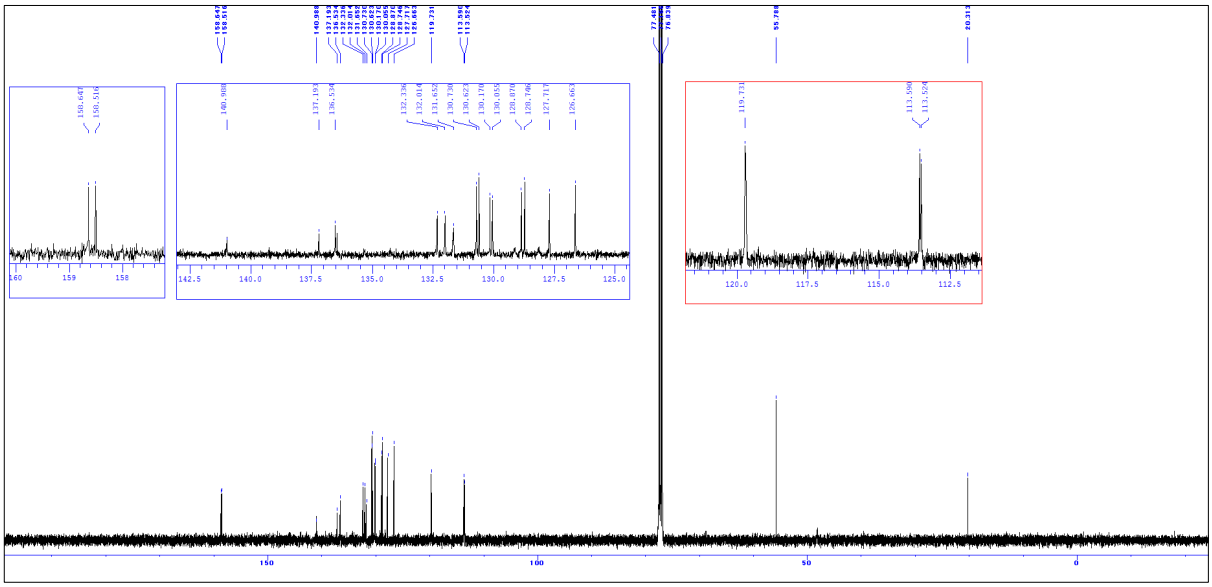

Fig. S23. $^{13}C\{^{1}H\}$ NMR spectrum of *trans*-**6aa-Me** (100 MHz, $CDCl_3$).

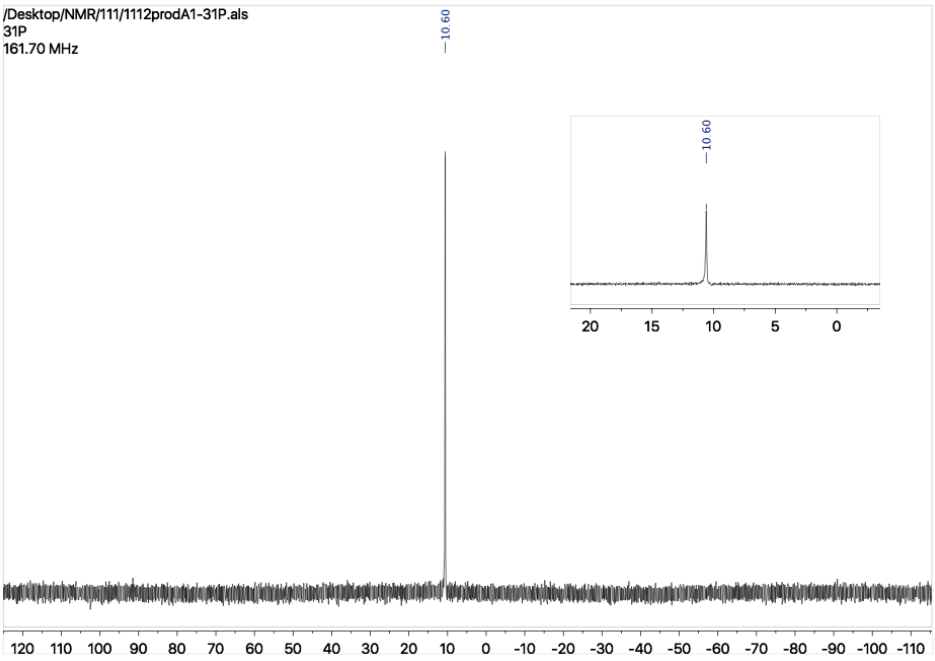

Fig. S24. $^{31}P\{^{1}H\}$ NMR spectrum of *trans*-**6aa-Me** (162 MHz, $CDCl_3$).

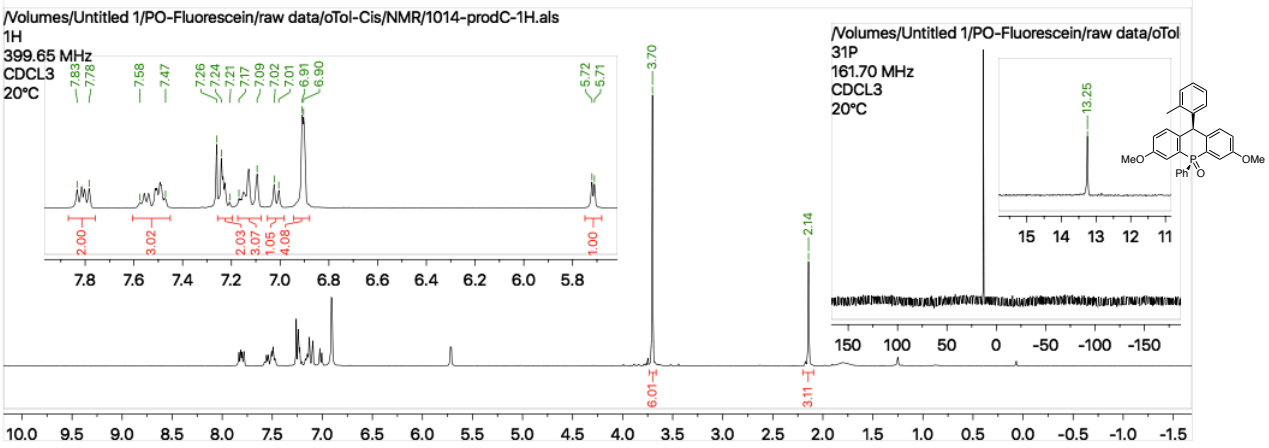

Fig. S25. ^{1}H NMR (400 MHz, $CDCl_3$) and $^{31}P\{^{1}H\}$ NMR (inset: 162 MHz, $CDCl_3$) spectra of *cis*-**6aa-Me**.

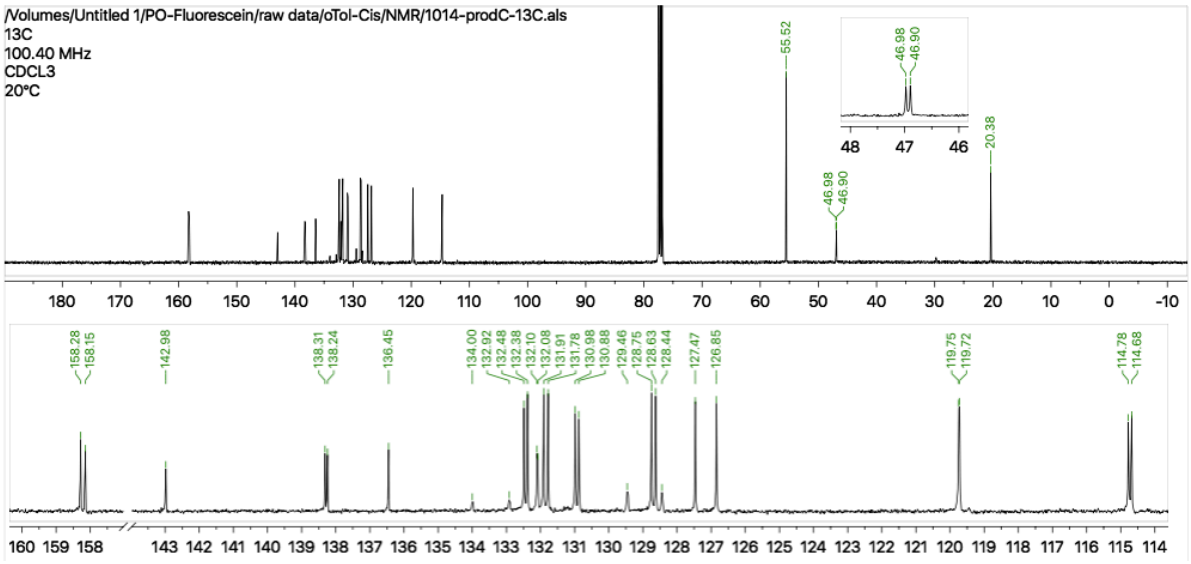

Fig. S26. $^{13}C\{^{1}H\}$ NMR spectra of *cis*-**6aa-Me** (100 MHz, $CDCl_3$).

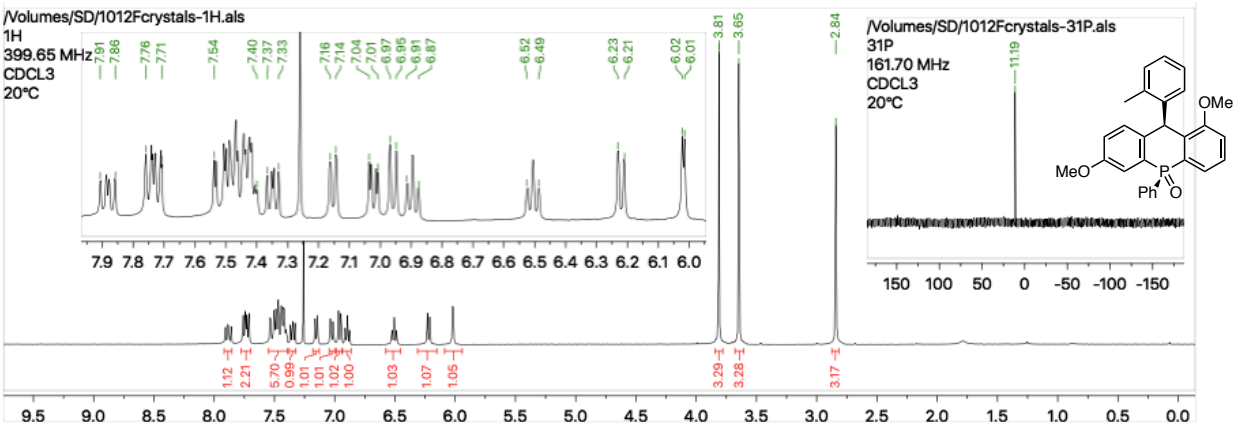

Fig. S27. ^{1}H NMR (400 MHz, $CDCl_3$) and $^{31}P\{^{1}H\}$ NMR (inset: 162 MHz, $CDCl_3$) spectra of *cis*-**6ab-Me**.

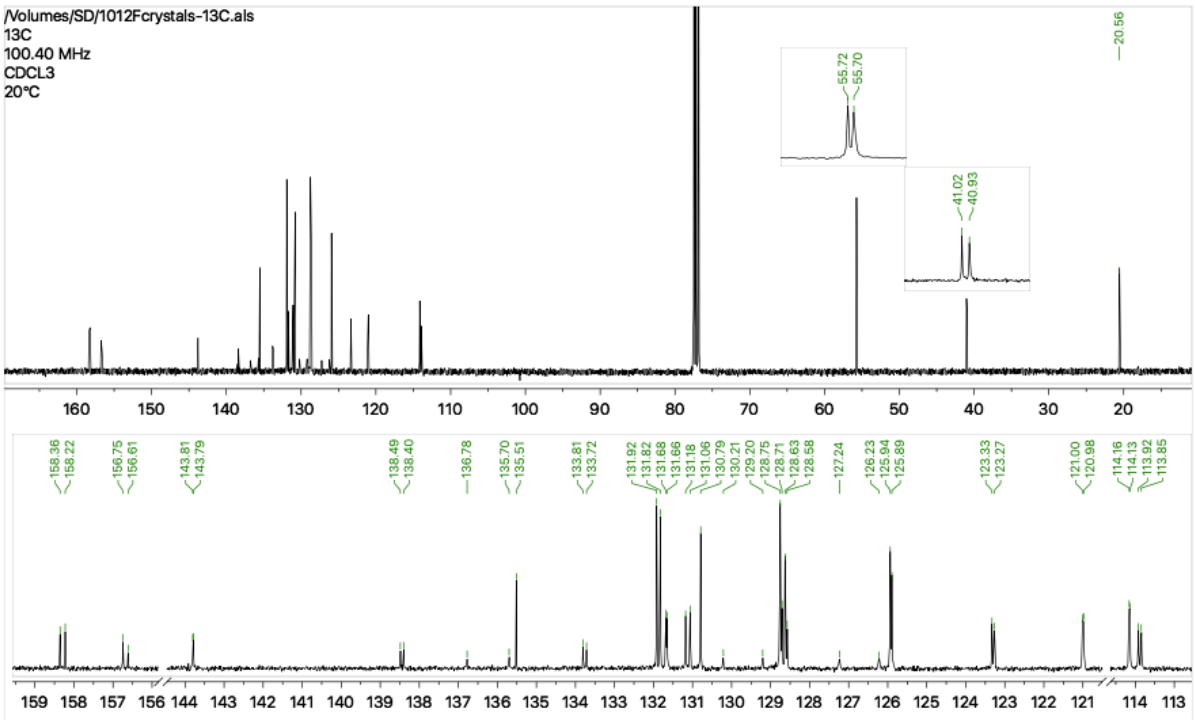

Fig. S28. $^{13}C\{^{1}H\}$ NMR spectra of *cis*-**6ab-Me** (100 MHz, $CDCl_3$).

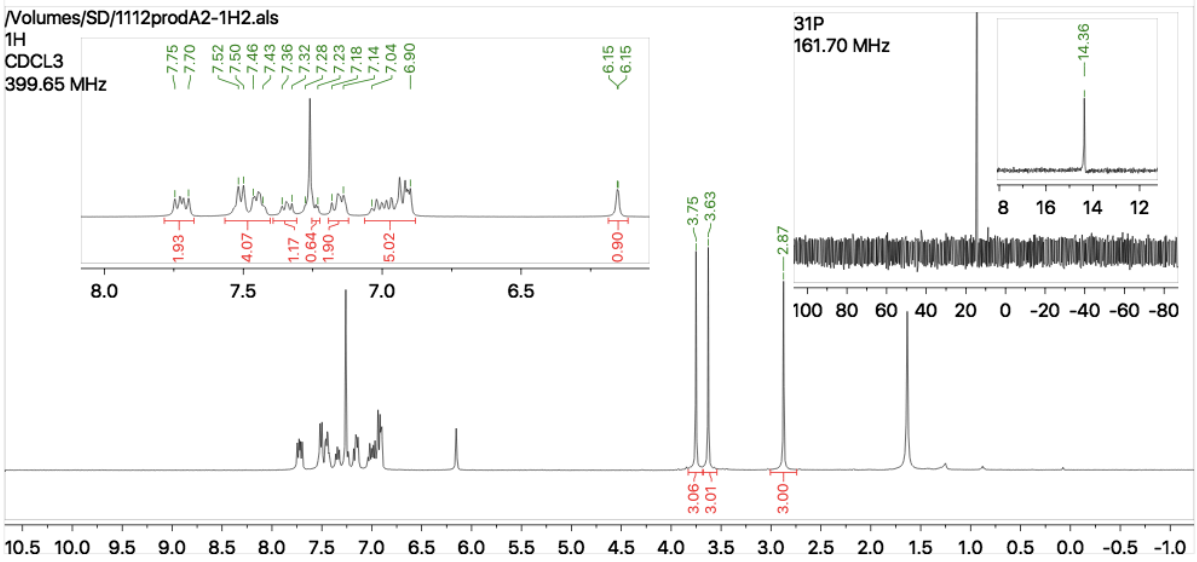

Fig. S29. ^{1}H NMR (400 MHz, $CDCl_3$) and $^{31}P\{^{1}H\}$ NMR (inset: 162 MHz, $CDCl_3$) spectra of *trans*-**6ab-Me**.

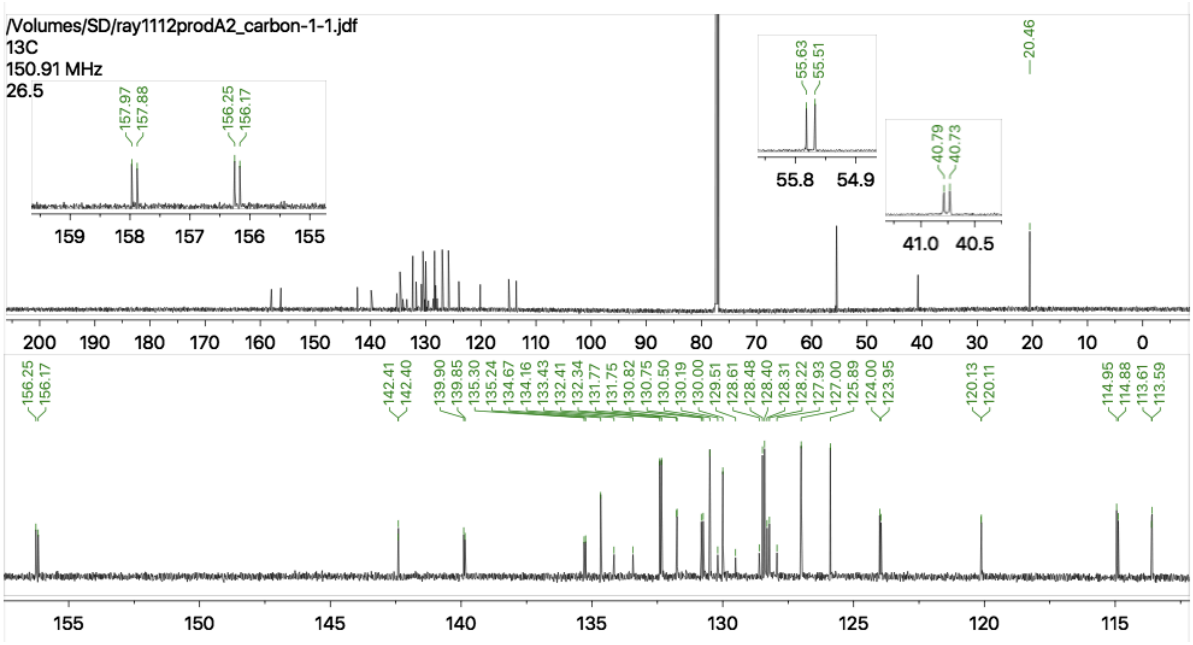

Fig. S30. $^{13}C\{^{1}H\}$ NMR spectra of *trans*-**6ab-Me** (100 MHz, $CDCl_3$).

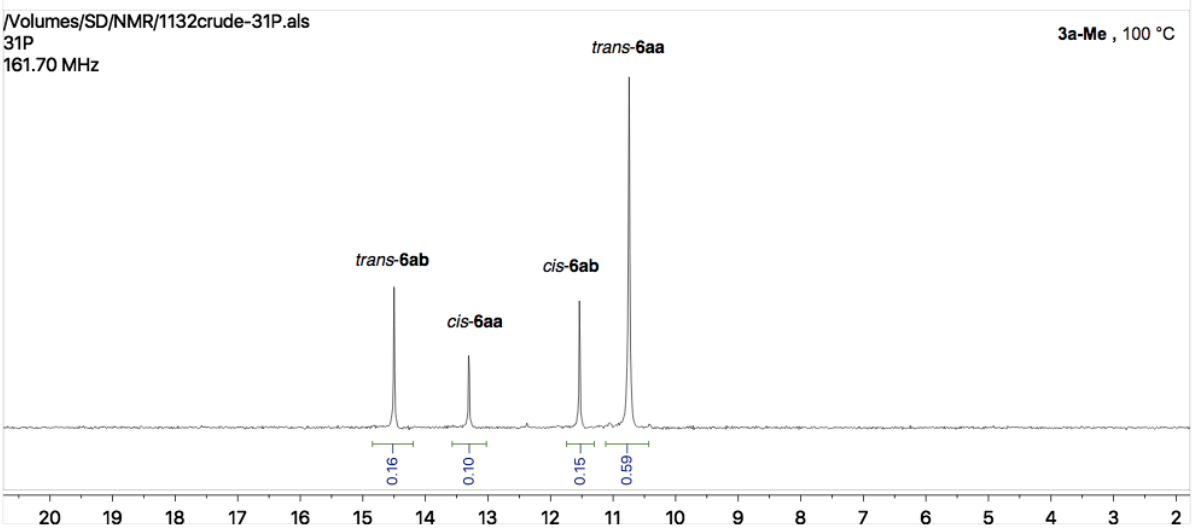

Fig. S31. $^{31}P\{^{1}H\}$ NMR spectrum of the crude reaction mixture after the cyclization of *in-situ*-generated **3a-Me** at 100 °C (162 MHz, $CDCl_3$). The assignment of signals are based on the $^{31}P\{^{1}H\}$ NMR spectra of each isolated product.

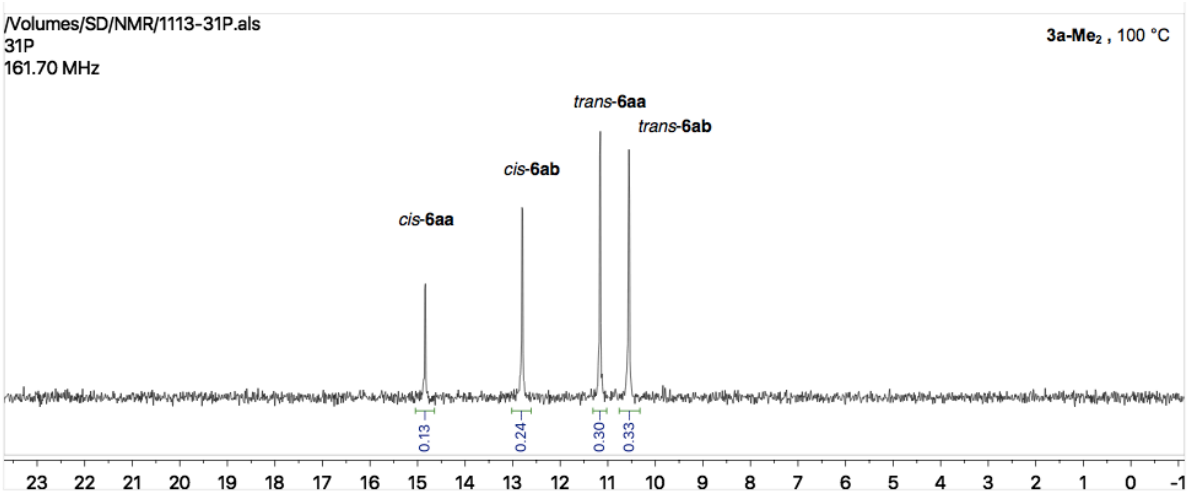

Fig. S32. $^{31}P\{^{1}H\}$ NMR spectrum of the crude reaction mixture after the cyclization of *in-situ*-generated **3a-Me$_2$** at 100 °C (162 MHz, $CDCl_3$).

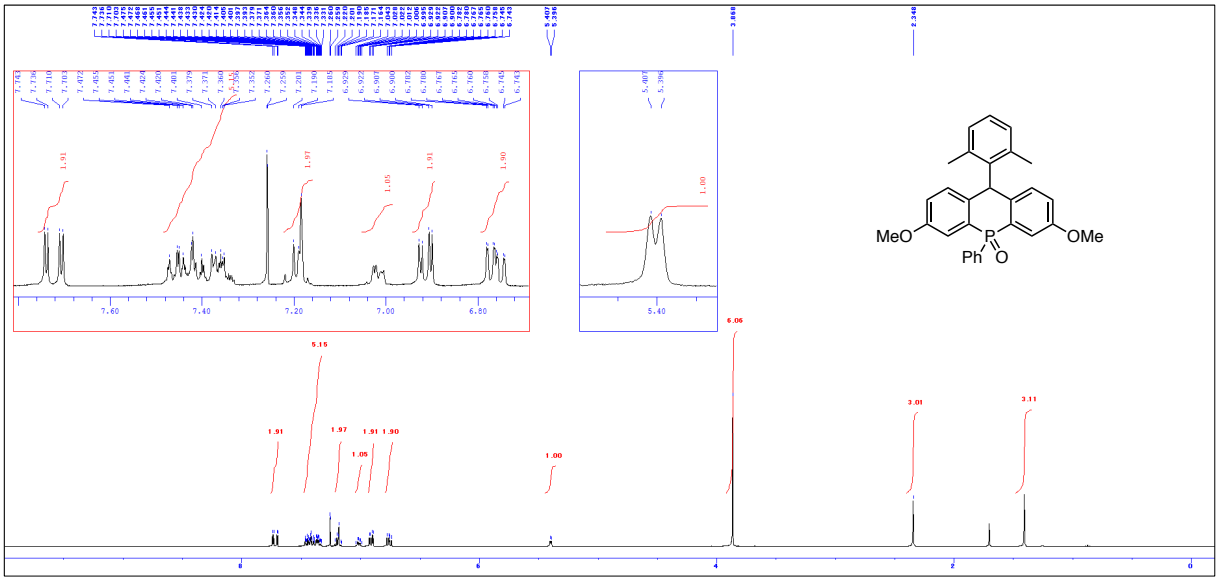

Fig. S33. ^{1}H NMR spectrum of *trans*-**6aa-Me$_2$** (400 MHz, $CDCl_3$).

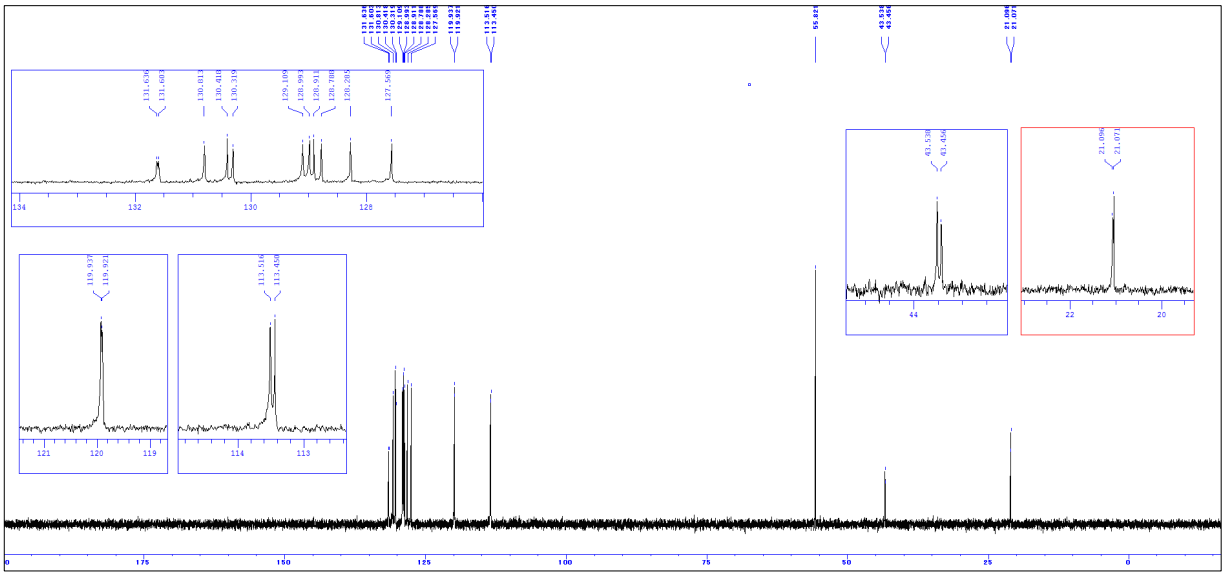

Fig. S34. $^{13}C\{^{1}H\}$ NMR spectrum of *trans*-**6aa-Me$_2$** (100 MHz, $CDCl_3$).

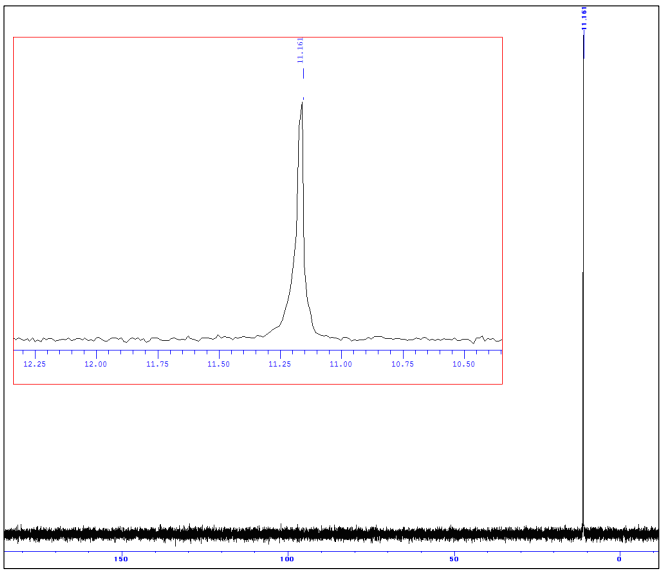

Fig. S35. $^{31}P\{^{1}H\}$ NMR spectrum of *trans*-**6aa-Me$_2$** (162 MHz, $CDCl_3$).

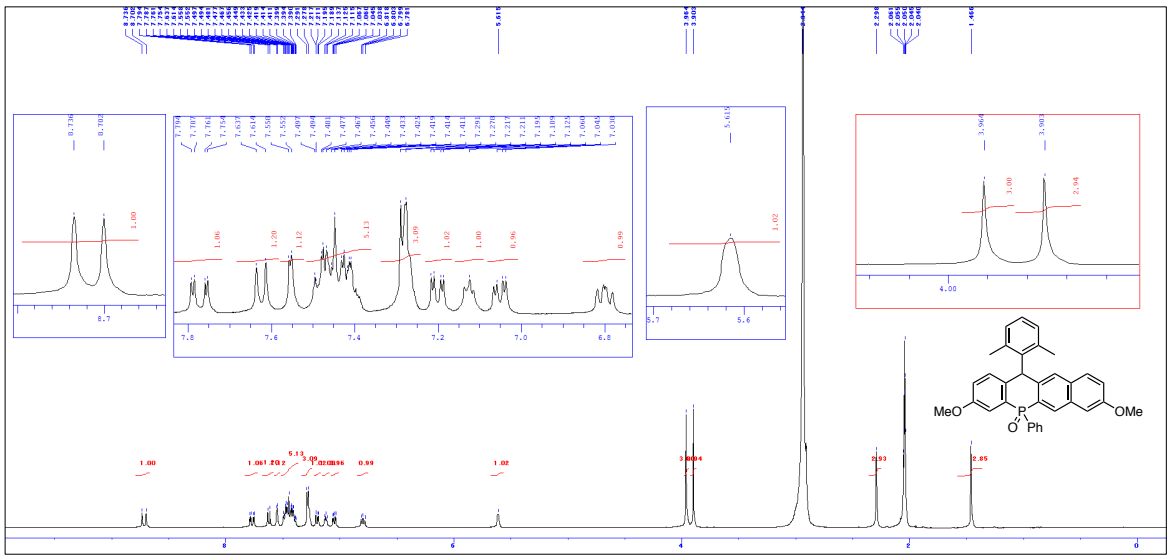

Fig. S36. ^{1}H NMR spectrum of *trans*-**6ba-Me$_2$** (400 MHz, acetone-d_6).

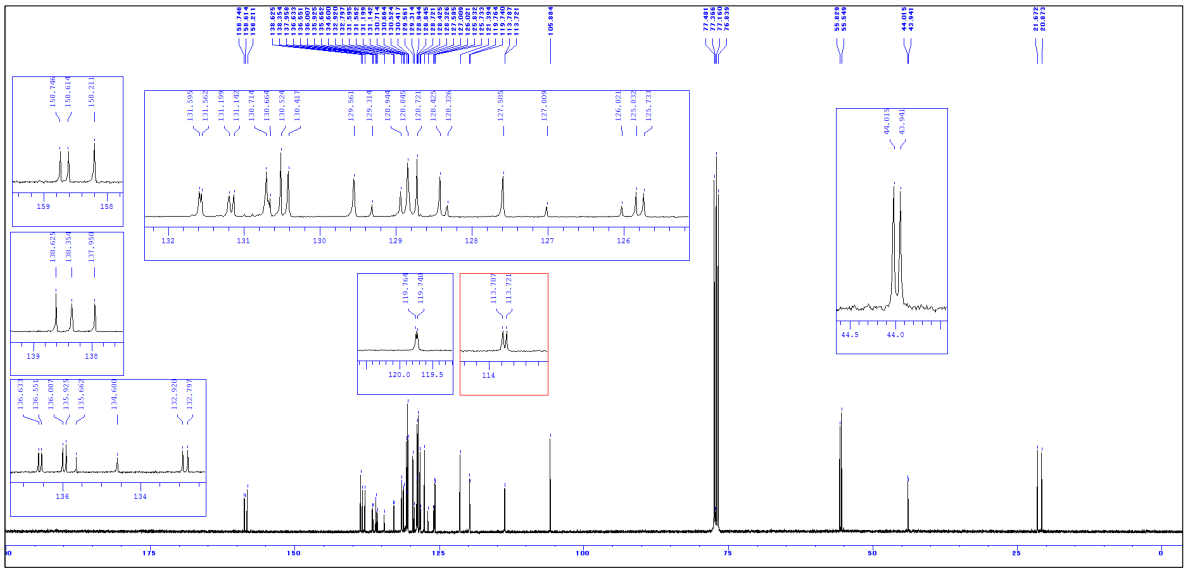

Fig. S37. ^{13}C{^{1}H} NMR spectrum of ***trans*-6ba-Me$_2$** (100 MHz, $CDCl_3$).

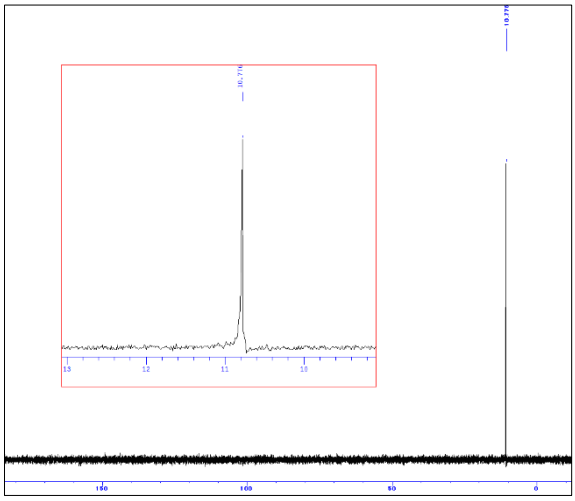

Fig. S38. $^{31}P\{^{1}H\}$ NMR spectrum of *trans*-**6ba-Me$_2$** (162 MHz, $CDCl_3$).

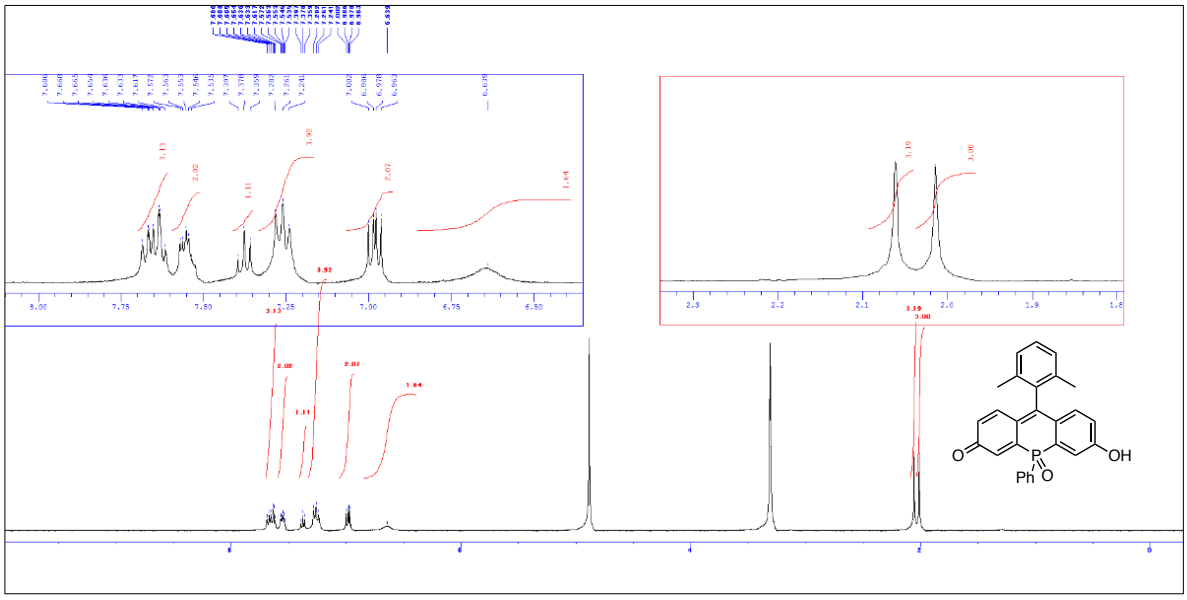

Fig. S39. ^{1}H NMR spectrum of POF-Me_2 (400 MHz, methanol-d_4).

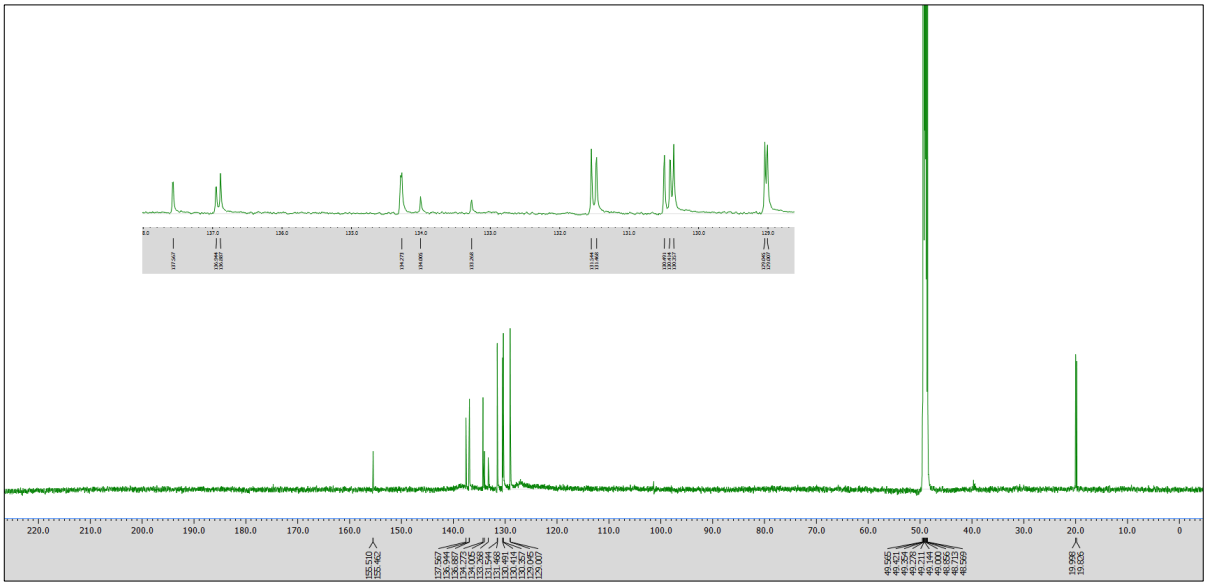

Fig. S40. $^{13}C\{^{1}H\}$ NMR spectrum of POF-Me_2 (150 MHz, methanol-d_4).

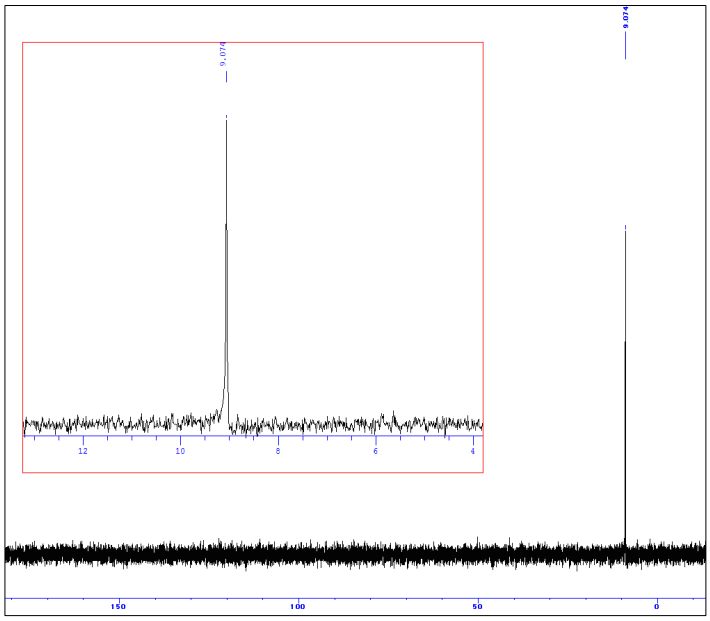

Fig. S41. $^{31}P\{^{1}H\}$ NMR spectrum of POF-Me_2 (162 MHz, methanol-d_4).

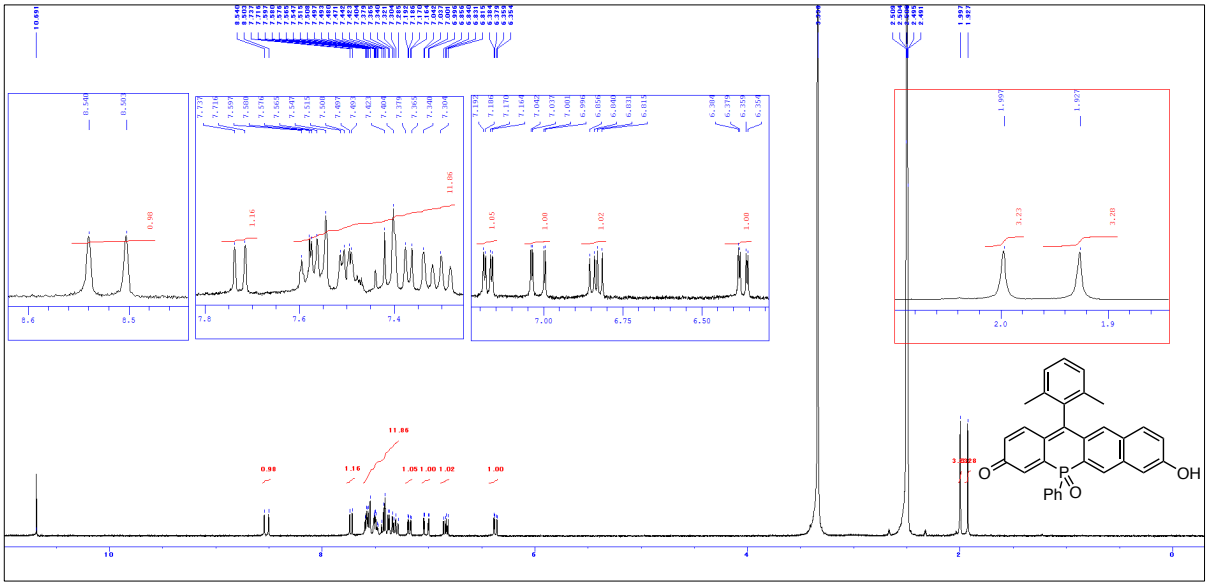

Fig. S42. ^{1}H NMR spectrum of SNAPF-Me$_2$ (400 MHz, DMSO-d_6).

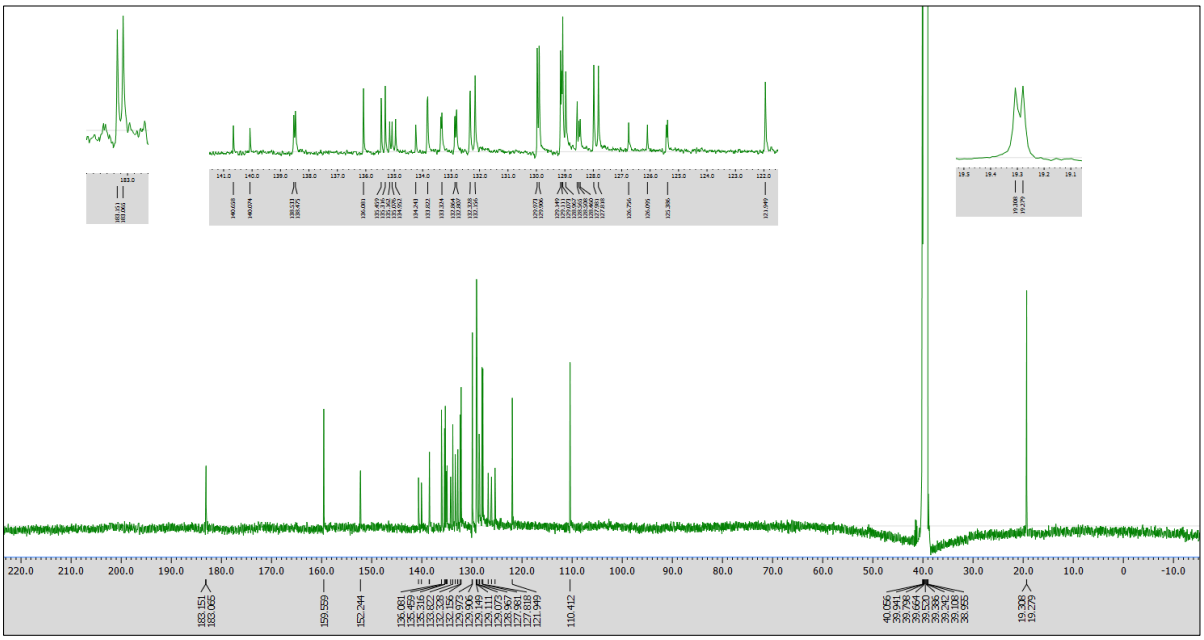

Fig. S43. ^{13}C{^{1}H} NMR spectrum of SNAPF-Me$_2$ (150 MHz, DMSO-d_6).

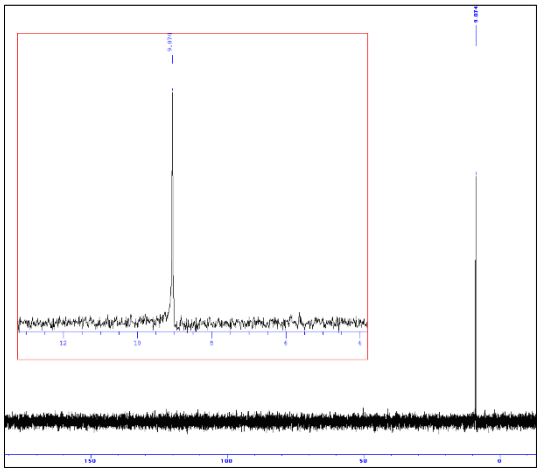

Fig. S44. $^{31}P\{^{1}H\}$ NMR spectrum of SNAPF-Me_2 (162 MHz, DMSO-d_6).

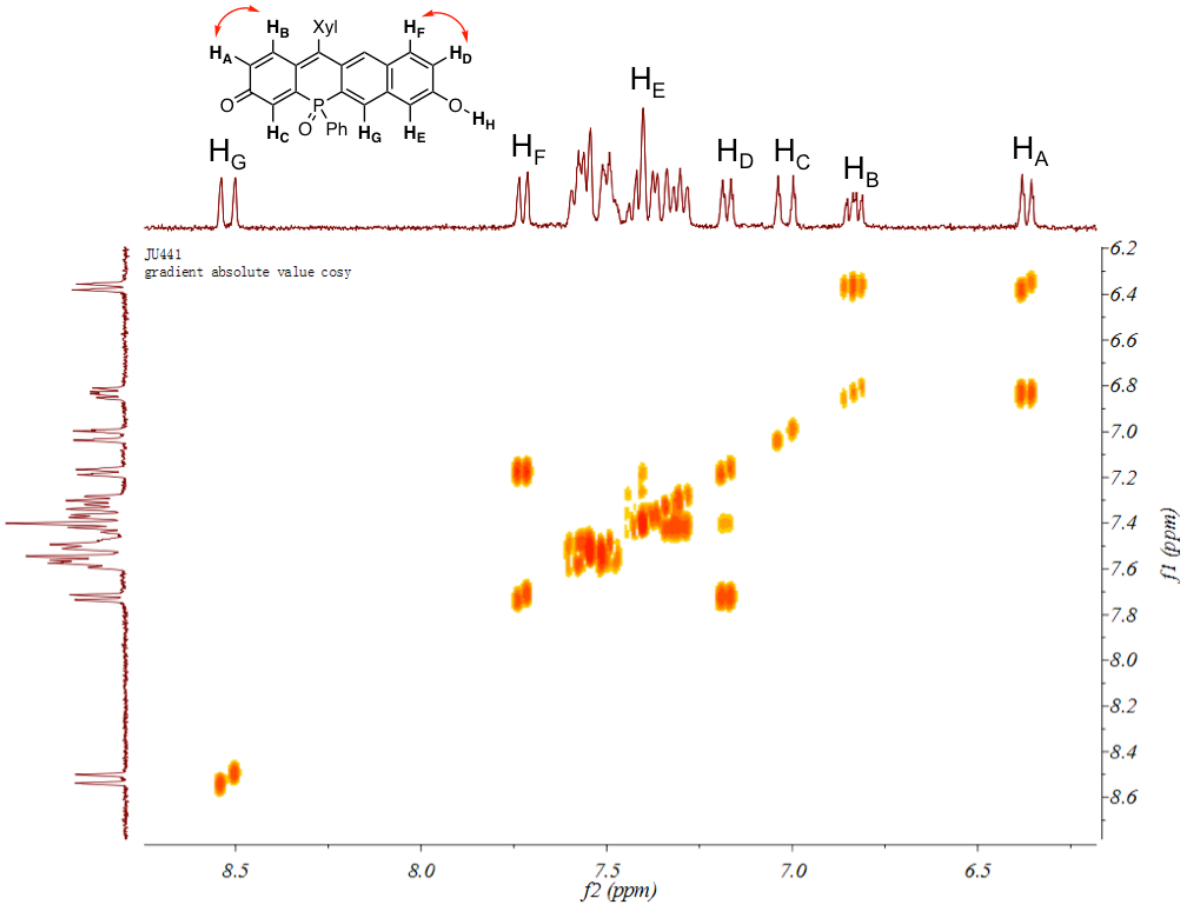

Fig. S45. H–H COSY 2D NMR spectrum of SNAPF-Me_2 (400 MHz, DMSO-d_6).

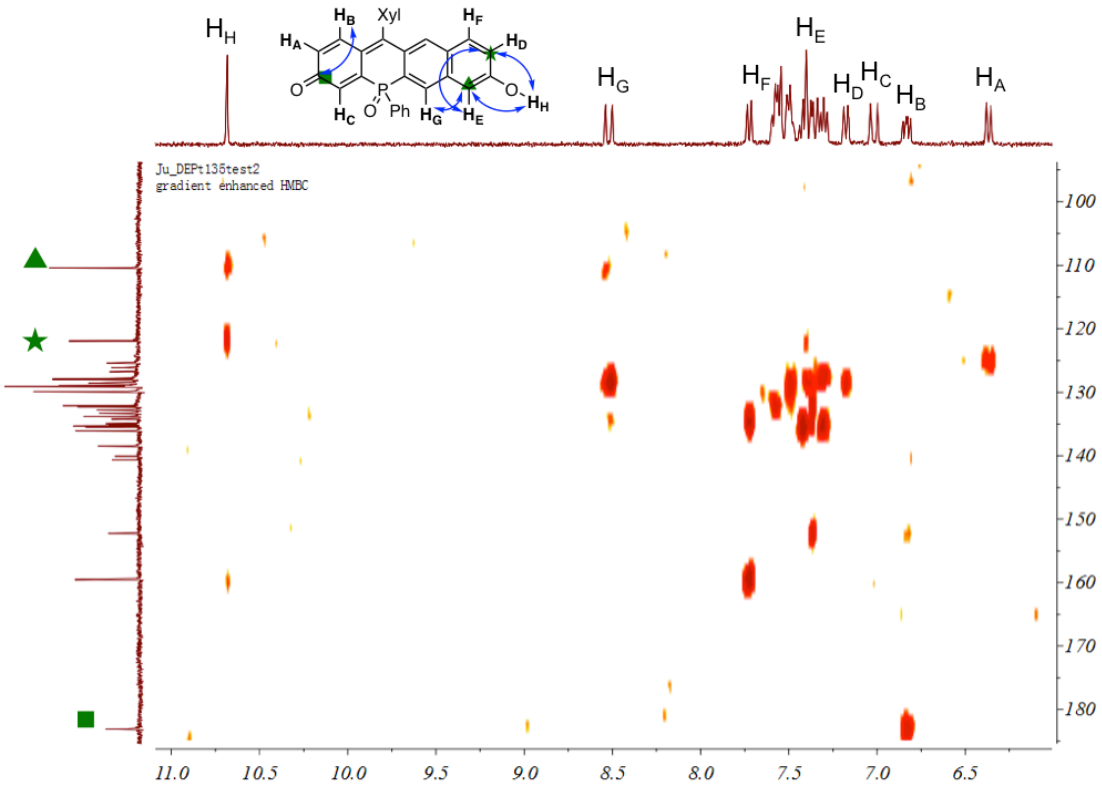

Fig. S46. HMBC 2D-NMR spectrum of SNAPF-Me_2 (400 MHz, DMSO-d_6).

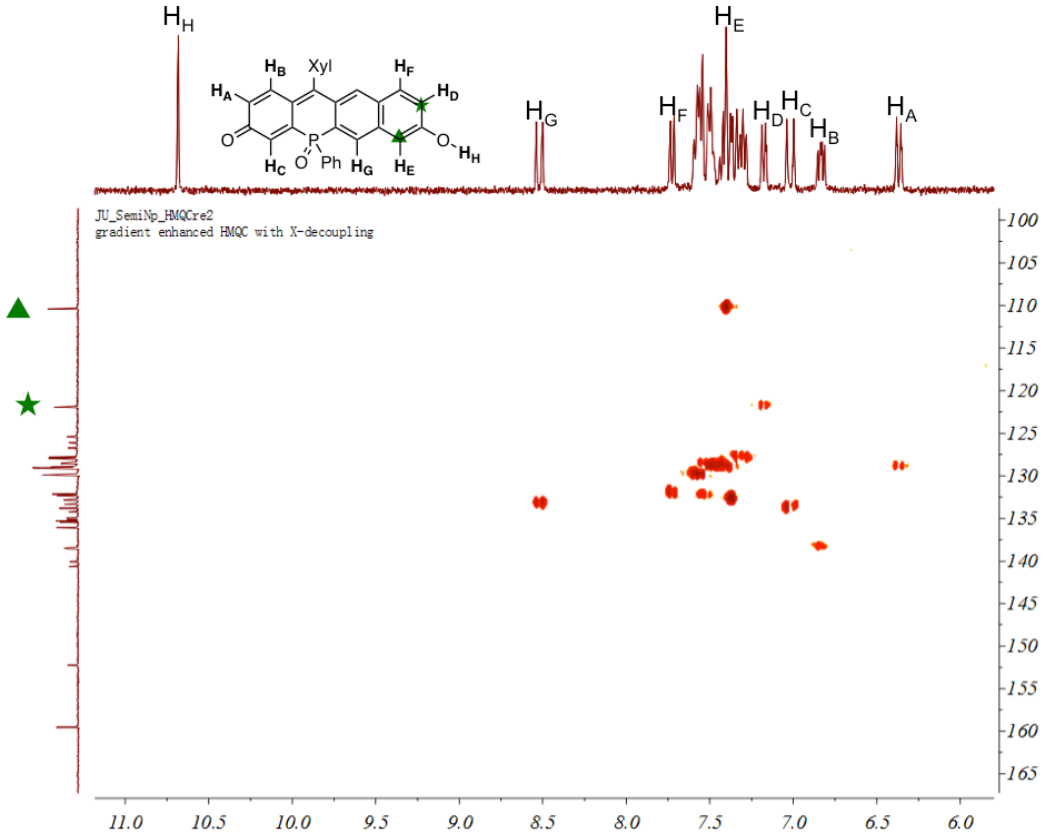

Fig. S47. HMQC 2D-NMR spectrum of SNAPF-Me_2 (400 MHz, DMSO-d_6).

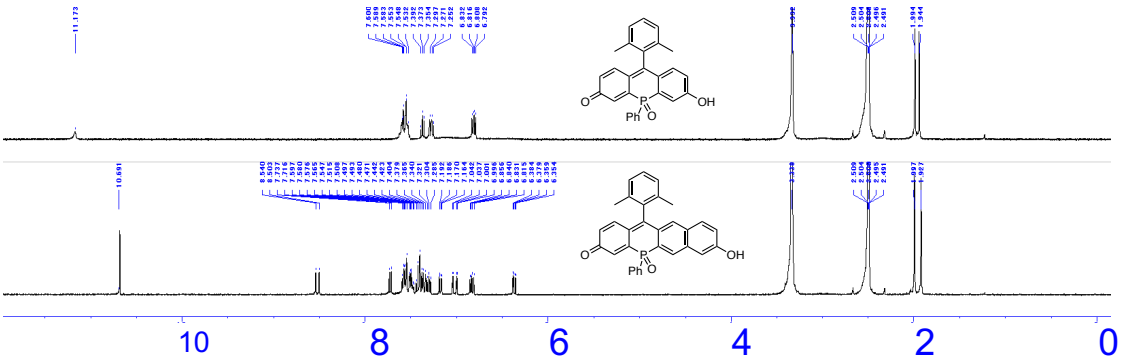

Fig. S48. Comparison of ^{1}H NMR spectra of POF-Me_2 (top) and SNAPF-Me_2 (bottom) (400 MHz, DMSO-d_6).